Understanding Negative Samples in Instance Discriminative Self-supervised Representation Learning

Kento Nozawa
The University of Tokyo & RIKEN AIP
nzw@g.ecc.u-tokyo.ac.jp

Issei Sato
The University of Tokyo
sato@g.ecc.u-tokyo.ac.jp

Abstract

Instance discriminative self-supervised representation learning has been attracted attention thanks to its unsupervised nature and informative feature representation for downstream tasks. In practice, it commonly uses a larger number of negative samples than the number of supervised classes. However, there is an inconsistency in the existing analysis; theoretically, a large number of negative samples degrade classification performance on a downstream supervised task, while empirically, they improve the performance. We provide a novel framework to analyze this empirical result regarding negative samples using the coupon collector's problem. Our bound can implicitly incorporate the supervised loss of the downstream task in the self-supervised loss by increasing the number of negative samples. We confirm that our proposed analysis holds on real-world benchmark datasets.

1 Introduction

Self-supervised representation learning is a popular class of unsupervised representation learning algorithms in the domains of vision [Bachman et al., 2019, Chen et al., 2020a, He et al., 2020, Caron et al., 2020, Grill et al., 2020, Chen and He, 2021] and language [Mikolov et al., 2013, Devlin et al., 2019, Brown et al., 2020]. Generally, it trains a feature extractor by solving a pretext task constructed on a large unlabeled dataset. The learned feature extractor yields generic feature representations for other machine learning tasks such as classification. Recent self-supervised representation learning algorithms help a linear classifier to attain classification accuracy comparable to a supervised method from scratch, especially in a few amount of labeled data regime [Newell and Deng, 2020, Hénaff et al., 2020, Chen et al., 2020b]. For example, `SwAV` [Caron et al., 2020] with ResNet-50 has a top-1 validation accuracy of 75.3% on the ImageNet-1K classification [Deng et al., 2009] compared with 76.5% by using the fully supervised method.

InfoNCE [van den Oord et al., 2018, Eq. 4] or its modification is a de facto standard loss function used in many state-of-the-art self-supervised methods [Logeswaran and Lee, 2018, Bachman et al., 2019, He et al., 2020, Chen et al., 2020a, Hénaff et al., 2020, Caron et al., 2020]. Intuitively, the minimization of InfoNCE can be viewed as the minimization of cross-entropy loss on $K+1$ instance-wise classification, where K is the number of negative samples. Despite the empirical success of self-supervised learning, we still do not understand why the self-supervised learning algorithms with InfoNCE perform well for downstream tasks.

Arora et al. [2019] propose the first theoretical framework for contrastive unsupervised representation learning (CURL). However, there exists a gap between the theoretical analysis and empirical observation as in Figure 1. Precisely, we expect that a large number of negative samples degrade a supervised loss on a downstream task from the analysis by Arora et al. [2019]. In practice, however,

35th Conference on Neural Information Processing Systems (NeurIPS 2021).

a large number of negative samples are commonly used in self-supervised representation learning algorithms [He et al., 2020, Chen et al., 2020a].

Contributions. We show difficulty to explain why large negative samples empirically improve supervised accuracy on the downstream task from the CURL framework when we use learned representations as feature vectors for the supervised classification in Section 3. To fill the gap, we propose a novel lower bound to theoretically explain this empirical observation regarding negative samples using the coupon collector's problem in Section 4.

2 InfoNCE-based Self-supervised Representations Learning

We focus on Chen et al. [2020a]'s self-supervised representation learning formulation, namely, SimCLR.[1] Let X be an input space, e.g., $X \subseteq \mathbb{R}^{\text{channel} \times \text{width} \times \text{height}}$ for color images. We can only access a unlabeled training dataset $\{\mathbf{x}_i\}_{i=1}^N$, where input $\mathbf{x} \in X$. SimCLR learns feature extractor $\mathbf{f} : X \to \mathbb{R}^h$ modeled by neural networks on the dataset, where h is the dimensionality of feature representation. Let $\mathbf{z} = \mathbf{f}(\mathbf{a}(\mathbf{x}))$ that is a feature representation of $\mathbf{x}$ after applying data augmentation $\mathbf{a} : X \to X$. Data augmentation is a pre-defined stochastic function such as a composition of the horizontal flipping and cropping. Note that the output of $\mathbf{f}$ is normalized by its L2 norm. Let $\mathbf{z}^+ = \mathbf{f}(\mathbf{a}^+(\mathbf{x}))$ that is a positive feature representation created from $\mathbf{x}$ with different data augmentation $\mathbf{a}^+(\cdot)$.

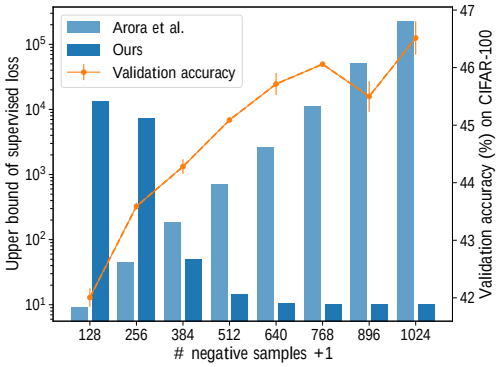

Figure 1: Upper bounds of supervised loss and validation accuracy on CIFAR-100. By increasing the number of negative samples, validation accuracy tends to improve. **Left bars**: The existing contrastive unsupervised representation learning bound (8) also increases when the number of negative samples increases because the bound of supervised loss explodes due to a collision term that is not related to classification loss (see Eq. (8) for the definition). **Right bars with ★**: On the other hand, the proposed counterpart (10) does not explode. Section 5 describes the details of this experiment.

SimCLR minimizes the following InfoNCE-based loss with K negative samples for each pair of $(\mathbf{z}, \mathbf{z}^+)$:

$$\ell_{\mathsf{Info}}(\mathbf{z}, \mathbf{Z}) := \ln \frac{\exp(\mathbf{z} \cdot \mathbf{z}^+/t)}{\sum_{\mathbf{z}_k \in \mathbf{Z}} \exp(\mathbf{z} \cdot \mathbf{z}_k/t)}, \tag{1}$$

where $\mathbf{Z} = \{\mathbf{z}^+, \mathbf{z}_1, \ldots, \mathbf{z}_K\}$ that is a set of positive representation $\mathbf{z}^+$ and K negative representations $\{\mathbf{z}_1, \ldots, \mathbf{z}_K\}$ created from other samples, $(\cdot \cdot)$ is an inner product of two representations, and $t \in \mathbb{R}_+$ is a temperature parameter.[2] Intuitively, this loss function approximates an instance-wise classification loss by using K random negative samples [Wu et al., 2018]. From the definition of Eq. (1), we expect that $\mathbf{f}$ learns an invariant encoder with respect to data augmentation $\mathbf{a}$. After minimizing Eq. (1), $\mathbf{f}$ works as a feature extractor for downstream tasks such as classification.

3 Extension of Contrastive Unsupervised Representation Learning Framework

We focus on the direct relationship between the self-supervised loss and a supervised loss to understand the role of the number of negative samples K. For a similar problem, the CURL framework [Arora et al., 2019] shows that the averaged supervised loss is bounded by the contrastive unsupervised loss. Thus, we extend the analysis of CURL to the self-supervised representation learning in Section 2 and point out that we have difficulty explaining the empirical observation as

[1] In fact, our theoretical analysis is valid with asymmetric feature extractors such as MoCo [He et al., 2020], where the positive and negative features do not come from feature extractor $\mathbf{f}$.

[2] We perform the analysis with $t = 1$ for simplicity, but our analysis holds with any temperature.

in Figure 1 from the existing analysis. Table 2 in Appendix A summarizes notations used in this paper for convenience.

3.1 CURL Formulation for SimCLR

By following the CURL analysis [Arora et al., 2019], we introduce the learning process in two steps: *self-supervised representation learning step* and *supervised learning step* (see Section 3.1.1 and Section 3.1.2, respectively).

3.1.1 Self-supervised representation learning step

The purpose of the self-supervised learning step is to learn a feature extractor $\mathbf{f}$ on an unlabeled dataset. During this step, we can only access input samples from X without any relationship between samples, unlike metric learning [Kulis, 2012] or similar unlabeled learning [Bao et al., 2018].

We formulate the data generation process for Eq. (1). The key idea of the CURL analysis is the existence of latent classes C that are associated with supervised classes.[3] Let ρ be a probability distribution over C, and let $\mathbf{x}$ be an input sample drawn from a data distribution D_c conditioned on a latent class $c \in C$. We draw two data augmentations $(\mathbf{a}, \mathbf{a}^+)$ from the distribution of data augmentation A and apply them independently to the sample. As a result, we have two augmented samples $(\mathbf{a}(\mathbf{x}), \mathbf{a}^+(\mathbf{x}))$ and call $\mathbf{a}^+(\mathbf{x})$ as a positive sample of $\mathbf{a}(\mathbf{x})$. Similarly, we draw K negative samples from D_{c_k} for each $c_k \in \{c_1, \dots, c_K\} \quad \rho^K$ and K data augmentations from A, and then we apply them to negative samples. Definition 1 summarizes the data generation process. Note that we suppose data augmentation $\mathbf{a} \quad A$ does not change the latent class of $\mathbf{x} \in X$.

Definition 1 (Data Generation Process in Self-supervised Representation Learning Step)**.**
1. Draw latent classes: $c, \{c_k\}_{k=1}^K \quad \rho^{K+1}$; *2. Draw input sample:* $\mathbf{x} \quad D_c$;
3. Draw data augmentations: $(\mathbf{a}, \mathbf{a}^+) \quad A^2$; *4. Apply data augmentations:* $\mathbf{a}(\mathbf{x}), \mathbf{a}^+(\mathbf{x})$;
5. Draw negative samples: $\{\mathbf{x}_k\}_{k=1}^K \quad D_{c_k}^K$; *6. Draw data augmentations:* $\{\mathbf{a}_k\}_{k=1}^K \quad A^K$;
7. Apply data augmentations: $\{\mathbf{a}_k(\mathbf{x}_k)\}_{k=1}^K$.

Note that the original data generation process of CURL samples a positive sample of $\mathbf{x}$ from D_c independently and does not use any data augmentations.

From the data generation process and InfoNCE loss (1), we give the following formal definition of self-supervised loss.

Definition 2 (Expected Self-supervised Loss)**.**

$$L_{\mathsf{Info}}(\mathbf{f}) \coloneqq \mathop{\mathsf{E}}_{c, \{c_k\}_{k=1}^K \quad \rho^{K+1}} \mathop{\mathsf{E}}_{\substack{\mathbf{x} \quad D_c \\ (\mathbf{a}, \mathbf{a}^+) \quad A^2}} \mathop{\mathsf{E}}_{\substack{\{\mathbf{x}_k\} \quad D_{c_k} \\ \{\mathbf{a}_k\}_{k=1}^K \quad A^K}} \ell_{\mathsf{Info}}(\mathbf{z}, \mathbf{Z}), \tag{2}$$

where recall that $\mathbf{z} = \mathbf{f}(\mathbf{a}(\mathbf{x}))$ *and* $\mathbf{Z} = \{\mathbf{f}(\mathbf{a}^+(\mathbf{x})), \mathbf{f}(\mathbf{a}_1(\mathbf{x}_1)), \dots, \mathbf{f}(\mathbf{a}_K(\mathbf{x}_K))\}$.

Since we cannot directly minimize Eq. (2), we minimize the empirical counterpart, $\widehat{L}_{\mathsf{Info}}(\mathbf{f})$, by sampling from the training dataset. After minimizing $\widehat{L}_{\mathsf{Info}}(\mathbf{f})$, learned $\widehat{\mathbf{f}}$ works as a feature extractor in the supervised learning step.

3.1.2 Supervised learning step

At the supervised learning step, we can observe label $y \in Y = \{1, \dots, Y\}$ for each $\mathbf{x}$ that is used in the self-supervised learning step. Let S be a supervised data distribution over $X \quad Y$, and $\mathbf{g} \quad \widehat{\mathbf{f}} : X \to \mathsf{R}^Y$ be a classifier, where $\mathbf{g} : \mathsf{R}^h \to \mathsf{R}^Y$ and $\widehat{\mathbf{f}}$ is the frozen feature extractor. Given the

[3] Technically, we do not need c to draw $\mathbf{x}$ for self-supervised representation learning. However, we explicitly include it in the data generation process to understand the relationship with a supervised task in Section 3.2. In the main analysis, we assume that the supervised classes in the downstream task are subset of C; however, different relationship between supervised and latent classes is discussed in Appendix B.

supervised data distribution and classifier, our goal is to minimize the following supervised loss:

$$L_{\mathsf{sup}}(\mathbf{g} \quad \widehat{\mathbf{f}}) \coloneqq \mathop{\mathsf{E}}_{\substack{\mathbf{x},y \\ \mathbf{a}}} \mathop{S}_{A} \quad \ln \frac{\exp\left(\mathbf{g}_y(\widehat{\mathbf{f}}(\mathbf{a}(\mathbf{x})))\right)}{\sum_{j 2 Y} \exp\left(\mathbf{g}_j(\widehat{\mathbf{f}}(\mathbf{a}(\mathbf{x})))\right)}. \tag{3}$$

By following the CURL analysis, we introduce a mean classifier as a simple instance of $\mathbf{g}$ because its loss is an upper bound of Eq. (3).[4] The mean classifier is the linear classifier whose weight of label y is computed by averaging representations: $\boldsymbol{\mu}_y = \mathsf{E}_{\mathbf{x} \quad D_y} \mathsf{E}_{\mathbf{a} \quad A} \mathbf{f}(\mathbf{a}(\mathbf{x}))$, where D_y is a data distribution conditioned on the supervise label y. We introduce the definition of the mean classifier's supervised loss as follows:

Definition 3 (Mean Classifier's Supervised Loss)**.**

$$L^{\mu}_{\mathsf{sup}}(\widehat{\mathbf{f}}) \coloneqq \mathop{\mathsf{E}}_{\substack{\mathbf{x},y \\ \mathbf{a}}} \mathop{S}_{A} \quad \ln \frac{\exp\left(\widehat{\mathbf{f}}(\mathbf{a}(\mathbf{x})) \quad \boldsymbol{\mu}_y\right)}{\sum_{j 2 Y} \exp\left(\widehat{\mathbf{f}}(\mathbf{a}(\mathbf{x})) \quad \boldsymbol{\mu}_j\right)}. \tag{4}$$

We also introduce a sub-class loss function.[5] Let Y_{sub} be a subset of Y and S_{sub} be a data distribution over $X \quad Y_{\mathsf{sub}}$, then we define the sub-class losses of classifier $\mathbf{g}$ and mean classifier:

Definition 4 (Supervised Sub-class Losses of Classifier $\mathbf{g}$ and Mean Classifier with $\widehat{\mathbf{f}}$)**.**

$$L_{\mathsf{sub}}(\mathbf{g} \quad \widehat{\mathbf{f}}, Y_{\mathsf{sub}}) \coloneqq \mathop{\mathsf{E}}_{\substack{\mathbf{x},y \\ \mathbf{a}}} \mathop{S_{\mathsf{sub}}}_{A} \quad \ln \frac{\exp\left(\mathbf{g}_y(\widehat{\mathbf{f}}(\mathbf{a}(\mathbf{x})))\right)}{\sum_{j 2 Y_{\mathsf{sub}}} \left(\mathbf{g}_j(\widehat{\mathbf{f}}(\mathbf{a}(\mathbf{x})))\right)}, \tag{5}$$

$$L^{\mu}_{\mathsf{sub}}(\widehat{\mathbf{f}}, Y_{\mathsf{sub}}) \coloneqq \mathop{\mathsf{E}}_{\substack{\mathbf{x},y \\ \mathbf{a}}} \mathop{S_{\mathsf{sub}}}_{A} \quad \ln \frac{\exp\left(\widehat{\mathbf{f}}(\mathbf{a}(\mathbf{x})) \quad \boldsymbol{\mu}_y\right)}{\sum_{j 2 Y_{\mathsf{sub}}} \exp\left(\widehat{\mathbf{f}}(\mathbf{a}(\mathbf{x})) \quad \boldsymbol{\mu}_j\right)}. \tag{6}$$

The purpose of unsupervised representation learning [Bengio et al., 2013] is to learn generic feature representation rather than improve the accuracy of the classifier on the same dataset. However, we believe that such a feature extractor tends to transfer well to another task. Indeed, Kornblith et al. [2019] empirically show a strong correlation between ImageNet's accuracy and transfer accuracy.

3.2 Theoretical Analysis based on CURL

We show that InfoNCE loss (2) is an upper bound of the expected sub-class loss of the mean classifier (6).

Step 1. Introduce a lower bound We denote $\boldsymbol{\mu}(\mathbf{x}) = \mathsf{E}_{\mathbf{a} \quad A} \mathbf{f}(\mathbf{a}(\mathbf{x}))$ and derive a lower bound of unsupervised loss $L_{\mathsf{Info}}(\mathbf{f})$.

$$\begin{aligned}
L_{\mathsf{Info}}(\mathbf{f}) & \mathop{\mathsf{E}}_{c, f c_k g_{k=1}^K \quad \rho^{K+1}} \quad \mathop{\mathsf{E}}_{\substack{\mathbf{x} \\ \mathbf{a}}} \mathop{D_c}_{A} f \mathbf{x}_k \quad \mathop{\mathsf{E}}_{D_{c_k} \; g_{k=1}^K} \ell_{\mathsf{Info}}\left(\mathbf{f}(\mathbf{a}(\mathbf{x})), \left\{\boldsymbol{\mu}(\mathbf{x}), \boldsymbol{\mu}(\mathbf{x}_1), \ldots, \boldsymbol{\mu}(\mathbf{x}_K)\right\}\right) \\
& \mathop{\mathsf{E}}_{c, f c_k g_{k=1}^K \quad \rho^{K+1}} \quad \mathop{\mathsf{E}}_{\substack{\mathbf{x} \\ \mathbf{a}}} \mathop{D_c}_{A} \ell_{\mathsf{Info}}\left(\mathbf{f}(\mathbf{a}(\mathbf{x})), \left\{\boldsymbol{\mu}(\mathbf{x}), \boldsymbol{\mu}_{c_1}, \ldots, \boldsymbol{\mu}_{c_K}\right\}\right) \\
& \mathop{\mathsf{E}}_{c, f c_k g_{k=1}^K \quad \rho^{K+1}} \quad \mathop{\mathsf{E}}_{\substack{\mathbf{x} \\ \mathbf{a}}} \mathop{D_c}_{A} \ell_{\mathsf{Info}}\left(\mathbf{f}(\mathbf{a}(\mathbf{x})), \left\{\boldsymbol{\mu}_c, \boldsymbol{\mu}_{c_1}, \ldots, \boldsymbol{\mu}_{c_K}\right\}\right) + d(\mathbf{f}),
\end{aligned} \tag{7}$$

$$\text{where } d(\mathbf{f}) = \frac{1}{t} \mathop{\mathsf{E}}_{c \; \rho_{\mathbf{x}}} \mathop{\mathsf{E}}_{D_c} \left\{ \mathop{\mathsf{E}}_{\mathbf{a} \quad A} \left[\mathbf{f}(\mathbf{a}(\mathbf{x}))\right] \quad \left[\mathop{\mathsf{E}}_{\substack{\mathbf{x}^+ \\ \mathbf{a}_1^+}} \mathop{D_c}_{A} \left[\mathbf{f}(\mathbf{a}_1^+(\mathbf{x}^+))\right] \right] \quad \mathop{\mathsf{E}}_{\mathbf{a}_2^+ \quad A} \left[\mathbf{f}(\mathbf{a}_2^+(\mathbf{x}))\right] \right\}.$$

[4] Concrete inequality is found in Appendix C.

[5] Arora et al. [2019] refer to this loss function as *averaged supervised loss*.

The first and second inequalities are done by using Jensen's inequality for convex function. The proof of the third inequality is shown in Appendix D.1. It is worth noting that positive and negative features can be extracted from another feature encoder or memory back He et al. [2020].

Remark 5 (Effect of gap term $d(\mathbf{f})$)**.** *We confirm that $d(\mathbf{f})$ is an almost constant among different K in practice (see Table 1). Therefore we focus on the first term in Eq.* (7) *in the following analysis.*

Step 2. Decomposition into the expected sub-class loss We convert the first term of Eq. (7) into the expected sub-class loss explicitly. By following Arora et al. [2019, Theorem B.1], we introduce collision probability: $\tau_K = \mathsf{P}(\mathrm{Col}(c, \{c_k\}_{k=1}^K) \neq 0)$, where $\mathrm{Col}(c, \{c_k\}_{k=1}^K) = \sum_{k=1}^K \mathsf{I}[c = c_k]$ and $\mathsf{I}[\,]$ is the indicator function. We omit the arguments of Col for simplicity. Let $\mathsf{C}_{\mathsf{sub}}(\{c, c_1, \ldots, c_K\})$ be a function to remove duplicated latent classes given latent classes. We omit the arguments of $\mathsf{C}_{\mathsf{sub}}$ as well. The result is our extension of Arora et al. [2019, Lemma 4.3] for self-supervised representation learning as the following proposition:

Proposition 6 (CURL Lower Bound of Self-supervised Loss)**.** *For all feature extractor $\mathbf{f}$,*

$$
\begin{aligned}
L_{\mathsf{Info}}(\mathbf{f}) \quad \geq (1 - \tau_K) \mathop{\mathsf{E}}_{c, \{c_k\}_{k=1}^K} \mathop{\mathsf{E}}_{\rho^{K+1}} [\underbrace{L^{\mu}_{\mathsf{sub}}(\mathbf{f}, \mathsf{C}_{\mathsf{sub}})}_{\textit{sub-class loss}} \mid \mathrm{Col} = 0] \\
+ \tau_K \mathop{\mathsf{E}}_{c, \{c_k\}_{k=1}^K} \mathop{\mathsf{E}}_{\rho^{K+1}} [\underbrace{\ln(\mathrm{Col} + 1)}_{\textit{collision}} \mid \mathrm{Col} \neq 0] + d(\mathbf{f}).
\end{aligned} \tag{8}
$$

The proof is found in Appendix D.2.

Arora et al. [2019] also show Rademacher complexity-based generalization error bound for the mean classifier. Since we focus on the behavior of the self-supervised loss rather than a generalization error bound when K increases, we do not perform further analysis as was done in Arora et al. [2019]. Nevertheless, we believe that constructing a generalization error bound by following either Arora et al. [2019, Theorem 4.1] or Nozawa et al. [2020, Theorem 7] is worth interesting future work.

3.3 Limitations of Eq. (8)

The bound (8) tells us that K gives a trade-off between the sub-class loss and collision term via τ_K. Recall that our final goal is to minimize the supervised loss (4) rather than expected sub-class loss (6). To incorporate the supervised loss (4) into the lower bound (8), we need K large enough to satisfy $\mathsf{C}_{\mathsf{sub}} \neq Y$. However, such a large K makes the lower bound meaningless.

We can easily observe that the lower bound (8) converges to the collision term by increasing K since the collision probability τ_K converges to 1. As a result, the sub-class loss rarely contributes to the lower bound. Let us consider the bound on CIFAR-10, where the number of supervised classes is 10, and latent classes are the same as the supervised classes. When $\tau_{K=32} \approx 0.967$, i.e., the only 3.3% training samples contribute to the expected sub-class loss, the others fall into the collision term. Indeed, Arora et al. [2019] show that small latent classes or large negative samples degrade classification performance of the expected sub-class classification task. However, even much larger negative samples, $K + 1 = 512$, yield the best performance of a linear classifier with self-supervised representation on CIFAR-10 [Chen et al., 2020a, B.9].

4 Proposed Lower Bound for Instance-wise Self-supervised Representation Learning

To fill the gap between the theoretical bound (8) and empirical observation from recent work, we propose another lower bound for self-supervised representation learning. The key idea of our bound is to replace τ with a different probability since τ can quickly increase depending on K. The idea is motivated by focusing on the supervised loss rather than the expected sub-class loss.

4.1 Proposed Lower Bound

Let υ_K be a probability that sampled K latent classes contain all latent classes: $\{c_k\}_{k=1}^K \supset C$. This probability appears in the coupon collector's problem of probability theory (e.g., Durrett [2019,

Example 2.2.7]). If the latent class probability is uniform: $\forall c, \rho(c) = 1/|\mathcal{C}|$, then we can calculate the probability explicitly as follows.

Definition 7 (Probability to Draw All Latent Classes)**.** *Assume that ρ is a uniform distribution over latent classes $\mathcal{C}$. The probability that K latent classes drawn from ρ contain all latent classes is defined as*

$$\upsilon_K := \sum_{n=1}^{K} \sum_{m=0}^{|\mathcal{C}|-1} \binom{|\mathcal{C}|}{m} (-1)^m \left(1 - \frac{m+1}{|\mathcal{C}|}\right)^n, \tag{9}$$

where the first summation is a probability that n drawn latent samples contain all latent classes [Nakata and Kubo, 2006, Eq. 2].[6]

By replacing τ with υ, we obtain our lower bound of InfoNCE loss:

Theorem 8 (Proposed Lower Bound of Self-supervised Loss)**.** *For all feature extractor $\mathbf{f}$,*

$$\begin{aligned} L_{\mathsf{Info}}(\mathbf{f}) \geq \frac{1}{2}\Big\{ & \upsilon_{K+1} \mathop{\mathbb{E}}_{c, \{c_k\}_{k=1}^{K}} \mathop{\mathbb{E}}_{\rho^{K+1}} [\underbrace{L^{\mu}_{\mathsf{sub}}(\mathbf{f}, \mathcal{C})}_{\text{sup. loss}} \mid \mathcal{C}_{\mathsf{sub}} = \mathcal{C}] \\ & + (1 - \upsilon_{K+1}) \mathop{\mathbb{E}}_{c, \{c_k\}_{k=1}^{K}} \mathop{\mathbb{E}}_{\rho^{K+1}} [\underbrace{L^{\mu}_{\mathsf{sub}}(\mathbf{f}, \mathcal{C}_{\mathsf{sub}})}_{\text{sub-class loss}} \mid \mathcal{C}_{\mathsf{sub}} \neq \mathcal{C}] \\ & + \mathop{\mathbb{E}}_{c, \{c_k\}_{k=1}^{K}} \mathop{\mathbb{E}}_{\rho^{K+1}} \underbrace{\ln(\mathrm{Col}+1)}_{\text{collision}} \Big\} + d(\mathbf{f}). \end{aligned} \tag{10}$$

The proof is found in Appendix D.3.

Theorem 8 tells us that probability υ_{K+1} converges to 1 by increasing the number of negative samples K; as a result, the self-supervised loss is more likely to contain the supervised loss and the collision term. The sub-class loss contributes to the self-supervised loss when K is small as in Eq. (8). Let us consider the example value of υ with the same setting discussed in Section 3.3. When $\upsilon_{K=32} \geq 0.719$, i.e., 71.9% training samples contribute the supervised loss.

4.2 Increasing K does not Spread Normalized Features within Same Latent Class

We argue that the feature representations do not have a large within-class variance on the feature space by increasing K in practice. To do so, we show the upper bound of the collision term in the lower bounds to understand the effect of large negative samples.

Corollary 9 (Upper Bound of Collision Term)**.** *Given a latent class c, K negative classes $\{c_k\}_{k=1}^{K}$, and feature extractor $\mathbf{f}$,*

$$\ln\left(\mathrm{Col}\left(c, \{c_k\}_{k=1}^{K}\right) + 1\right) \leq \alpha + \beta \mathop{\mathbb{E}}_{\substack{\mathbf{x} \sim D_c \\ (\mathbf{a}, \mathbf{a}^+) \sim A^2}} \mathop{\mathbb{E}}_{\substack{\mathbf{x}^0 \sim D_c \\ \mathbf{a}^0 \sim A}} \left\| \mathbf{f}(\mathbf{a}(\mathbf{x})) - \left[\mathbf{f}(\mathbf{a}^0(\mathbf{x}^0)) \quad \mathbf{f}(\mathbf{a}^+(\mathbf{x}))\right] \right\|, \tag{11}$$

where α and β are non-negative constants depending on the number of duplicated latent classes.

The proof is found in Appendix D.4. A similar bound is shown by Arora et al. [2019, Lemma 4.4].

Intuitively, we expect that two feature representations in the same latent class tend to be dissimilar by increasing K. However, Eq. (11) converges even if K is small in practice. Let us consider the condition when this upper bound achieves the maximum. Since $\mathbf{f}(\mathbf{a}(\mathbf{x}))$ and $\mathbf{f}(\mathbf{a}^+(\mathbf{x}))$ are computed from the same input sample with different data augmentations, their inner product tends to be 1; thus, $\mathbf{f}(\mathbf{a}^0(\mathbf{x}^0))$ is located in the opposite direction of $\mathbf{f}(\mathbf{a}(\mathbf{x}))$. But, it is not possible to learn such representations because of the definition of InfoNCE with normalized representation and the dimensionality of feature space: Equilateral dimension. We confirm that Eq. (11) without α and β does not increase by increasing K (see Table 1 and Appendix F for more analysis).

[6] We show expected $K+1$ to draw all supervised labels for ImageNet-1K and all used datasets in Appendix E.

4.3 Small K can Give Consistent Loss Function for Supervised Task

As we shown in Theorem 8, L_{Info} with large K can be viewed as an upper bound of L^{μ}_{sup}. However, L_{Info} with smaller K can still yield good feature representations for downstream tasks on ImageNet-1K as reported by Chen et al. [2020a]. Arora et al. [2019] also reported similar results on CIFAR-100 with contrastive losses.[7] To shed light on this smaller K regime, we focus on the class distributions of both datasets, ImageNet-1K and CIFAR-100, which are almost uniform.

Proposition 10 (Optimality of L_{sub})**.** *Suppose C Y and ρ is uniform: $\forall c \in \mathsf{C}, \rho(c) = 1/|\mathsf{C}|$. Suppose a constant function $\mathbf{q} : \mathbf{x} \in \mathcal{X} \mapsto \mathbf{q} \in \left[q_1, \dots, q_{|\mathsf{C}|}\right]^{\top}$. Optimal $\mathbf{q}$ is a constant function that outputs a vector with the same value if and only if it minimizes $\mathsf{E}_{c, \{\mathbf{z}_k\}_{k=1}^{K}} \rho^{K+1} L_{\mathsf{sub}}(\mathbf{q}, \mathsf{C}_{\mathsf{sub}})$. The optimal $\mathbf{q}$ is also the minimizer of L_{sup}.*

The proof is found in Appendix D.5 inspired by Titsias [2016, Proposition 2].

Proposition 10 *does not* argue that self-supervised representation learning algorithms fail to learn feature representations on a dataset with a non-uniform class distribution. This is because we perform a supervised algorithm on a downstream dataset after representation learning in general.

4.4 Relation to Clustering-based Self-supervised Representation Learning

During the minimization of L_{Info}, we cannot minimize L^{μ}_{sup} in Eq. (10) directly since we cannot access supervised and latent classes. Interestingly, we find a similar formulation in clustering-based self-supervised representation learning algorithms.

Remark 11. *Clustering-based self-supervised representation learning algorithms, such as* `DeepCluster` *[Caron et al., 2018],* `SeLa` *[Asano et al., 2020],* `SwAV` *[Caron et al., 2020], and* `PCL` *[Li et al., 2021a], use prototype representations instead of $\mathbf{z}^{+}, \{\mathbf{z}_k\}_{k=1}^{K}$ by applying unsupervised clustering on feature representations. This procedure is justified as the approximation of latent class's mean representation $\boldsymbol{\mu}_c$ with a prototype representation to minimize the supervised loss in Eq.* (10) *rather than Eq.* (2)*, as a result, the mini-batch size does not depend on the number of negative samples.*

This replacement supports the empirical observation in Caron et al. [2020, Section 4.3], where the authors reported `SwAV` maintained top-1 accuracy on ImageNet-1K with a small mini-batch size, 200, compared to a large mini-batch, $4\,096$. On the other hand, `SimCLR` [Chen et al., 2020a] did not.

5 Experiments

We numerically confirm our theoretical findings by using `SimCLR` [Chen et al., 2020a] on the image classification tasks. Appendix F contains NLP experiments and some analyses that have been omitted due to the lack of space. We used datasets with a relatively small number of classes to compare bounds. Our experimental codes are available online.[8]

Datasets and Data Augmentations We used the CIFAR-10 and CIFAR-100 [Krizhevsky, 2009] image classification datasets with the original $50\,000$ training samples for both self-supervised and supervised training and the original $10\,000$ validation samples for the evaluation of supervised learning. We used the same data augmentations in the CIFAR-10 experiment by Chen et al. [2020a]: random resize cropping with the original image size, horizontal flipping with probability 0.5, color jitter with a strength parameter of 0.5 with probability 0.8, and grey scaling with probability 0.2.

Self-supervised Learning We mainly followed the experimental setting provided by Chen et al. [2020a] and its implementation.[9] We used ResNet-18 [He et al., 2016] as a feature encoder without the last fully connected layer. We replaced the first convolution layer with the convolutional layer

[7] Arora et al. [2019, Table D.1] mentioned that this phenomenon is not covered by the CURL framework.

[8] `https://github.com/nzw0301/Understanding-Negative-Samples`. We used Hydra [Yadan, 2019], GNU Parallel [Tange, 2020], Scikit-learn [Pedregosa et al., 2011], Pandas [Reback et al., 2020], Matplotlib [Hunter, 2007], and seaborn [Waskom, 2021] in our experiments.

[9] `https://github.com/google-research/simclr`

with 64 output channels, the stride size of 1, the kernel size of 3, and the padding size of 3. We removed the first max-pooling from the encoder, and we added a non-linear projection head to the end of the encoder. The projection head consisted of the fully connected layer with 512 units, batch-normalization [Ioffe and Szegedy, 2015], ReLU activation function, and another fully connected layer with 128 units and without bias.

We trained the encoder by using PyTorch [Paszke et al., 2019]'s distributed data-parallel training [Li et al., 2020] on four GPUs, which are NVIDIA Tesla P100 on an internal cluster. For distributed training, we replaced all batch-normalization with synchronized batch-normalization. We used stochastic gradient descent with momentum factor of 0.9 on 500 epochs. We used LARC [You et al., 2017][10], and its global learning rate was updated by using linear warmup at each step during the first 10 epochs, then updated by using cosine annealing without restart [Loshchilov and Hutter, 2017] at each step until the end. We initialized the learning rate with $(K+1)/256$. We applied weight decay of 10^{-4} to all weights except for parameters of all synchronized batch-normalization and bias terms. The temperature parameter was set to $t = 0.5$.

Linear Evaluation We report the validation accuracy of two linear classifiers: mean classifier and linear classifier. We constructed a mean classifier by averaging the feature representations of $\mathbf{z}$ per supervised class. We applied one data augmentation to each training sample, where the data augmentation was the same as in that the self-supervised learning step. For linear classifier $\mathbf{g}$, we optimized $\mathbf{g}$ by using stochastic gradient descent with Nesterov's momentum [Sutskever et al., 2013] whose factor is 0.9 with 100 epochs. Similar to self-supervised training, we trained the classifier by using distributed data-parallel training on the four GPUs with 512 mini-batches on each GPU. The initial learning rate was 0.3, which was updated by using cosine annealing without restart [Loshchilov and Hutter, 2017] until the end.

Bound Evaluation We compared the extension bound of CURL (8) and our bound (10) by varying the number of negative samples K. We selected $K+1 \in \{32, 64, 128, 256, 512\}$ for CIFAR-10 and $K+1 \in \{128, 256, 384, 512, 640, 786, 896, 1024\}$ for CIFAR-100. After self-supervised learning, we approximated $\boldsymbol{\mu}_c$ by averaging 10 sampled data augmentations per sample on the training dataset and evaluated Equations (8) and (10) with the same negative sample size K as in self-supervised training.[11] We reported the averaged values over validation samples with 10 epochs: $(\lfloor 10\,000/(K+1) \rfloor \quad (K+1) \quad \text{epoch})$ pairs of $(\mathbf{z}, \mathbf{Z})$. Note that we used a theoretical value of υ defined by Eq. (9) to avoid dividing by zero if a realized υ value is 0. We also reported the upper bound of collision (11) without constants α, β referred to as "Collision Bound" on the training data. See Appendix F for details.

5.1 Experimental Results

Table 1 shows the bound values on CIFAR-10 and CIFAR-100. We only showed a part of values among different numbers of negative samples due to the page limitation.[12] We reported mean and linear classifiers' validation accuracy as "μ acc" and "Linear acc", respectively. As a reference, we reported practical linear evaluation's validation accuracy as "Linear acc w/o", where we discarded the non-linear projection head from the feature extractor [Chen et al., 2020a]. Since the CURL bound (8) does not contain ${}^{y}L^{\mu}_{\mathsf{sup}}$ explicitly, we subtracted ${}^{y}L^{\mu}_{\mathsf{sup}}$ from L^{μ}_{sub} in Eq. (8) and reported ${}^{y}L^{\mu}_{\mathsf{sup}}$ and subtracted L^{μ}_{sub} as ${}^{y}L^{\mu}_{\mathsf{sub}}$ for the comparison. We confirmed that CURL bounds converged to ^{y}Collision with relatively small K. On the other hand, proposed bound values had still a large proportion of supervised loss L^{μ}_{sup} with larger K. Figure 1 shows *upper* bounds of supervised loss L_{sup} and the linear accuracy by rearranging Equations (8) and (10). The reported values were averaged over three training runs of both self-supervised and supervised steps with different random seeds. The error bars represented the standard deviation.

[10] https://github.com/NVIDIA/apex

[11] Precisely, $\boldsymbol{\mu}_c = \frac{1}{N_c} \sum_{i=1}^{N} \mathsf{I}[y_i = c] \frac{1}{10} \sum_{j=1}^{10} \mathbf{f}(\mathbf{a}_j(\mathbf{x}_i))$.

[12] Tables 4 and 5 in Appendix F provides the comprehensive results.

Table 1: The bound values on CIFAR-10/100 experiments with different $K + 1$. CURL bound and its quantities are shown with y. The proposed ones are shown without y. Since the proposed collision values are half of ^{y}Collision, they are omitted. The reported values contain their coefficient except for Collision bound.

		CIFAR-10				CIFAR-100			
K + 1		32	128	256	512	128	256	512	1024
τ		0.96	1.00	1.00	1.00	0.72	0.92	0.99	1.00
υ		0.69	1.00	1.00	1.00	0.00	0.00	0.62	1.00
μ acc		72.75	77.22	78.60	80.12	32.67	34.25	35.90	37.44
Linear acc		77.13	81.33	82.85	84.13	41.95	43.53	45.16	46.57
Linear acc w/o		82.02	85.43	86.68	87.66	57.92	58.91	59.30	59.46
L_{Info}	Eq. (2)	2.02	3.29	3.96	4.64	3.32	3.98	4.66	5.34
$d(\mathbf{f})$	Eq. (7)	1.16	1.18	1.18	1.19	0.99	0.98	0.97	0.95
${}^{y}L_{\mathsf{Info}}$ bound	Eq. (8)	0.23	1.41	2.08	2.75	0.72	0.46	0.78	1.42
^{y}Collision		1.32	2.58	3.26	3.94	0.69	1.15	1.73	2.37
${}^{y}L^{\mu}_{\mathsf{sup}}$		0.05	0.00	0.00	0.00	0.00	0.00	0.01	0.00
${}^{y}L^{\mu}_{\mathsf{sub}}$		0.01	0.00	0.00	0.00	1.03	0.30	0.01	0.00
L_{Info} bound	Eq. (10)	0.39	1.02	1.35	1.69	1.18	1.53	1.86	2.19
L^{μ}_{sup}		0.63	0.91	0.90	0.90	0.00	0.00	1.17	1.94
L^{μ}_{sub}		0.26	0.00	0.00	0.00	1.82	1.93	0.79	0.01
Collision bound	Eq. (11)	0.60	0.61	0.62	0.62	0.52	0.52	0.51	0.51

6 Related Work

6.1 Self-supervised Representation Learning

Self-supervised learning tries to learn an encoder that extracts generic feature representations from an unlabeled dataset. Self-supervised learning algorithms solve a pretext task that does not require any supervision and can be easily constructed on the dataset, such as denoising [Vincent et al., 2008], colorization [Zhang et al., 2016, Larsson et al., 2016] solving jigsaw puzzles [Noroozi and Favaro, 2016], inpainting blank pixels [Pathak et al., 2016], reconstructing missing channels [Zhang et al., 2017], predicting rotation [Gidaris et al., 2018], and adversarial generative models [Donahue and Simonyan, 2019] for vision; predicting neighbor words [Mikolov et al., 2013], generating neighbor sentences [Kiros et al., 2015], and solving masked language model [Devlin et al., 2019] for language. See also recent review articles [Le-Khac et al., 2020, Schmarje et al., 2021].

Recent self-supervised learning algorithms for the vision domain mainly solve an instance discrimination task. `Exemplar-CNN` [Dosovitskiy et al., 2014] is one of the earlier algorithms that can obtain generic feature representations of images by using convolutional neural networks and data augmentation. After van den Oord et al. [2018] proposed InfoNCE loss function, many state-of-the-art self-supervised algorithms minimize InfoNCE-based loss function, e.g., `DeepInfoMax` [Hjelm et al., 2019], `AMDIM` [Bachman et al., 2019], `SimCLR` [Chen et al., 2020a], `CPCv2` [Hénaff et al., 2020], `MoCo` [He et al., 2020], and `SwAV` [Caron et al., 2020].

6.2 Theoretical Perspective

InfoNCE [van den Oord et al., 2018] was initially proposed as a lower bound of intractable mutual information between feature representations by using noise-contrastive estimation (NCE) [Gutmann and Hyvärinen, 2012]. Optimizing InfoNCE can be considered as maximizing the InfoMax principle [Linsker, 1988]. The history of InfoMax-based self-supervised representation learning dates back to more than 30 years ago [Hinton and Becker, 1990]. However, this interpretation does not directly explain the generalization for a downstream task. Indeed, Tschannen et al. [2020] empirically showed that the performances of classification on downstream tasks and mutual information estimation are uncorrelated with each other. Kolesnikov et al. [2019] also reported a similar relationship between the performances of linear classification on downstream tasks and of pretext tasks. McAllester and Stratos [2020] theoretically showed the limitation of maximizing the lower bounds of mutual information – accurate approximation requires an exponential sample size.

As the most related work, Arora et al. [2019] provide the first theoretical analyses to explain the generalization of the CURL. It is worth noting that our analysis focuses on the different representation learning setting. Shortly after our publishing a draft of this paper on arXiv, Ash et al. [2021] also

published a paper on the role of negative samples in CURL bound with InfoNCE loss for fully supervised classification using the coupon collector's problem. Thus we believe that the coupon collector's problem is a key ingredient to analyze the connection between contrastive learning and supervised classification based on the CURL analysis by Arora et al. [2019]. Their work was developed independently of ours and their analysis is for contrastive unsupervised learning rather than self-supervised learning that is done in this work. The proposed bound by Ash et al. [2021] has also similar issue to Arora et al. [2019] as in our analysis; however, their bound holds with smaller K than C. Bansal et al. [2021] decomposed the generalization error gap of a linear classifier given feature representations. Wang and Isola [2020] decomposed the self-supervised loss into alignment and uniformity and showed properties of both metrics. Li et al. [2021b] provided an interpretation of InfoNCE through a lens of kernel method. Mitrovic et al. [2021] provided another theoretical analysis with causality for instance discriminative self-supervised learning. Tosh et al. [2021] also analyzed self-supervised loss for augmented samples, but they only focused on one negative sample setting. Recently, Wei et al. [2021] proposed learning theoretical analysis by introducing "expansion" assumption for self-training where (pseudo) labels are generated from the previously learned model. Learning theory-based analyses were also proposed for other types of self-supervised learning problem such as reconstruction task [Garg and Liang, 2020, Lee et al., 2021] and language modeling [Saunshi et al., 2021]. The theoretical analysis on self-supervised representation algorithms without negative samples [Tian et al., 2021] cannot be applied to the contrastive learning setting.

6.3 Hard Negative Mining

In metric learning and contrastive learning, hard negative mining, such as Kalantidis et al. [2020], is actively proposed to make training more effective to avoid using inappropriate negative or too easy negative samples. The current work mainly focuses on the *quality* of negative samples rather than *quantity* of negative samples. However, removing false-negative samples can reduce the effect of the collision term in our bounds. Thus our analysis might provide a theoretical justification for hard negative mining.

7 Conclusion

We applied the CURL framework to the recent self-supervised representation learning formulation. We pointed out that the existing framework has difficulty explaining why large negative samples in self-supervised learning improve classification accuracy on a downstream supervised task as in Figure 1. We proposed a novel framework using the coupon collector's problem to explain the phenomenon and confirmed our analysis on real-world benchmark datasets.

Limitations We did not discuss the properties of data augmentation explicitly in our framework. Practically, self-supervised representation learning algorithms discard the projection head after self-supervised learning, but our analysis does not cover this procedure. We believe that extensions to cover these settings are fruitful explorations of future work.

Acknowledgments

This work is supported (in part) by Next Generation AI Research Center, The University of Tokyo. The experiments were conducted using the SGI Rackable C2112-4GP3/C1102-GP8 (Reedbush-H/L) in the Information Technology Center, The University of Tokyo. We thank Han Bao, Yoshihiro Nagano, and Ikko Yamane for constructive discussion and Yusuke Tsuzuku for supporting our experiments. We also thank Junya Honda and Yivan Zhang for LaTeX support, specifically, for solving our font issue and MathJax, respectively. We appreciate anonymous reviewers of ICML 2021 and NeurIPS 2021 for giving constructive suggestions to improve our manuscript. KN is supported by JSPS KAKENHI Grant Number 18J20470.

References

S. Arora, H. Khandeparkar, M. Khodak, O. Plevrakis, and N. Saunshi. A Theoretical Analysis of Contrastive Unsupervised Representation Learning. In *ICML*, pages 5628–5637, 2019.

Y. M. Asano, C. Rupprecht, and A. Vedaldi. Self-labelling via Simultaneous Clustering and Representation Learning. In *ICLR*, 2020.

J. T. Ash, S. Goel, A. Krishnamurthy, and D. Misra. Investigating the Role of Negatives in Contrastive Representation Learning. *arXiv:2106.09943v1 [cs.LG]*, 2021.

P. Bachman, R. D. Hjelm, and W. Buchwalter. Learning Representations by Maximizing Mutual Information Across Views. In *NeurIPS*, pages 15535–15545, 2019.

Y. Bansal, G. Kaplun, and B. Barak. For Self-Supervised Learning, Rationality Implies Generalization, Provably. In *ICLR*, 2021.

H. Bao, G. Niu, and M. Sugiyama. Classification from Pairwise Similarity and Unlabeled Data. In *ICML*, pages 452–461, 2018.

Y. Bengio, A. Courville, and P. Vincent. Representation Learning: A Review and New Perspectives. *IEEE Transactions on Pattern Analysis and Machine Intelligence*, 35(8):1798–1828, 2013.

T. B. Brown, B. Mann, N. Ryder, M. Subbiah, J. Kaplan, P. Dhariwal, A. Neelakantan, P. Shyam, G. Sastry, A. Askell, S. Agarwal, A. Herbert-Voss, G. Krueger, T. Henighan, R. Child, A. Ramesh, D. M. Ziegler, J. Wu, C. Winter, C. Hesse, M. Chen, E. Sigler, M. Litwin, S. Gray, B. Chess, J. Clark, C. Berner, S. Mccandlish, A. Radford, I. Sutskever, and D. Amodei. Language Models are Few-Shot Learners. In *NeurIPS*, pages 1877–1901, 2020.

M. Caron, P. Bojanowski, A. Joulin, and M. Douze. Deep Clustering for Unsupervised Learning of Visual Features. In *ECCV*, pages 139–156, 2018.

M. Caron, I. Misra, J. Mairal, P. Goyal, P. Bojanowski, and A. Joulin. Unsupervised Learning of Visual Features by Contrasting Cluster Assignments. In *NeurIPS*, pages 9912–9924, 2020.

T. Chen, S. Kornblith, M. Norouzi, and G. Hinton. A Simple Framework for Contrastive Learning of Visual Representations. In *ICML*, pages 1597–1607, 2020a.

T. Chen, S. Kornblith, K. Swersky, M. Norouzi, and G. Hinton. Big Self-Supervised Models are Strong Semi-Supervised Learners. In *NeurIPS*, 2020b.

X. Chen and K. He. Exploring Simple Siamese Representation Learning. In *CVPR*, pages 15750–15758, 2021.

J. Deng, W. Dong, R. Socher, L.-J. Li, K. Li, and L. Fei-Fei. ImageNet: A Large-Scale Hierarchical Image Database. In *CVPR*, pages 248–255, 2009.

J. Devlin, M.-W. Chang, K. Lee, and K. Toutanova. BERT: Pre-training of Deep Bidirectional Transformers for Language Understanding. In *NAACL-HLT*, pages 4171–4186, 2019.

J. Donahue and K. Simonyan. Large Scale Adversarial Representation Learning. In *NeurIPS*, pages 10542–10552, 2019.

A. Dosovitskiy, P. Fischer, J. T. Springenberg, M. Riedmiller, and T. Brox. Discriminative Unsupervised Feature Learning with Convolutional Neural Networks. In *NeurIPS*, pages 766–774, 2014.

R. Durrett. *Probability: Theory and Examples*. Cambridge Series in Statistical and Probabilistic Mathematics. Cambridge University Press, 5 edition, 2019.

P. Flajolet, D. Gardy, and L. Thimonier. Birthday Paradox, Coupon Collectors, Caching Algorithms and Self-organizing Search. *Discrete Applied Mathematics*, 39(3):207–229, 1992.

T. Gao, X. Yao, and D. Chen. SimCSE: Simple Contrastive Learning of Sentence Embeddings. In *EMNLP*, 2021.

S. Garg and Y. Liang. Functional Regularization for Representation Learning: A Unified Theoretical Perspective. In *NeurIPS*, pages 17187–17199, 2020.

S. Gidaris, P. Singh, and N. Komodakis. Unsupervised Representation Learning by Predicting Image Rotations. In *ICLR*, 2018.

J.-B. Grill, F. Strub, F. Altché, C. Tallec, P. H. Richemond, E. Buchatskaya, C. Doersch, B. A. Pires, Z. D. Guo, M. G. Azar, B. Piot, K. Kavukcuoglu, R. Munos, and M. Valko. Bootstrap Your Own Latent A New Approach to Self-Supervised Learning. In *NeurIPS*, pages 21271–21284, 2020.

M. U. Gutmann and A. Hyvärinen. Noise-Contrastive Estimation of Unnormalized Statistical Models, with Applications to Natural Image Statistics. *Journal of Machine Learning Research*, 13:307–361, 2012.

K. He, X. Zhang, S. Ren, and J. Sun. Deep Residual Learning for Image Recognition. In *CVPR*, pages 770–778, 2016.

K. He, H. Fan, Y. Wu, S. Xie, and R. Girshick. Momentum Contrast for Unsupervised Visual Representation Learning. In *CVPR*, pages 9726–9735, 2020.

O. J. Hénaff, A. Srinivas, J. De Fauw, A. Razavi, C. Doersch, S. M. A. Eslami, and A. Van den oord. Data-Efficient Image Recognition with Contrastive Predictive Coding. In *ICML*, pages 4182–4192, 2020.

G. E. Hinton and S. Becker. An Unsupervised Learning Procedure that Discovers Surfaces in Random-dot Stereograms. In *IJCNN*, pages 218–222, 1990.

R. D. Hjelm, A. Fedorov, S. Lavoie-Marchildon, K. Grewal, P. Bachman, A. Trischler, and Y. Bengio. Learning Deep Representations by Mutual Information Estimation and Maximization . In *ICLR*, 2019.

J. D. Hunter. Matplotlib: A 2D graphics environment. *Computing in Science & Engineering*, 9(3):90–95, 2007. doi: 10.1109/MCSE.2007.55.

S. Ioffe and C. Szegedy. Batch Normalization: Accelerating Deep Network Training by Reducing Internal Covariate Shift. In *ICML*, pages 448–456, 2015.

A. Joulin, E. Grave, P. Bojanowski, and T. Mikolov. Bag of Tricks for Efficient Text Classification. In *EACL*, volume 2, pages 427–431, 2017.

Y. Kalantidis, M. B. Sariyildiz, N. Pion, P. Weinzaepfel, and D. Larlus. Hard Negative Mixing for Contrastive Learning. In *NeurIPS*, pages 21798–21809, 2020.

R. Kiros, Y. Zhu, R. Salakhutdinov, R. S. Zemel, A. Torralba, R. Urtasun, and S. Fidler. Skip-Thought Vectors. In *NeurIPS*, pages 3294–3302, 2015.

A. Kolesnikov, X. Zhai, and L. Beyer. Revisiting Self-Supervised Visual Representation Learning. In *CVPR*, pages 1920–1929, 2019.

S. Kornblith, J. Shlens, and Q. V. Le. Do Better ImageNet Models Transfer Better? In *CVPR*, pages 2661–2671, 2019.

A. Krizhevsky. Learning Multiple Layers of Features from Tiny Images. Technical report, 2009.

B. Kulis. Metric Learning: A Survey. *Foundations and Trends® in Machine Learning*, 5(4):287–364, 2012.

G. Larsson, M. Maire, and G. Shakhnarovich. Learning Representations for Automatic Colorization. In *ECCV*, pages 577–593, 2016.

P. H. Le-Khac, G. Healy, and A. F. Smeaton. Contrastive Representation Learning: A Framework and Review. *IEEE Access*, 8:193907–193934, 2020.

J. D. Lee, Q. Lei, N. Saunshi, and J. Zhuo. Predicting What You Already Know Helps: Provable Self-Supervised Learning. In *NeurIPS*, 2021.

J. Li, P. Zhou, C. Xiong, and S. C. Hoi. Prototypical Contrastive Learning of Unsupervised Representations. In *ICLR*, 2021a.

S. Li, Y. Zhao, R. Varma, O. Salpekar, P. Noordhuis, T. Li, A. Paszke, J. Smith, B. Vaughan, P. Damania, and S. Chintala. PyTorch Distributed: Experiences on Accelerating Data Parallel Training. In *VLDB*, pages 3005–3018, 2020.

Y. Li, R. Pogodin, D. J. Sutherland, and A. Gretton. Self-Supervised Learning with Kernel Dependence Maximization. In *NeurIPS*, 2021b.

R. Linsker. Self-Organization in a Perceptual Network. *Computer*, 21(3):105–117, 1988.

L. Logeswaran and H. Lee. An Efficient Framework for Learning Sentence Representations. In *ICLR*, 2018.

I. Loshchilov and F. Hutter. SGDR: Stochastic Gradient Descent with Warm Restarts. In *ICLR*, 2017.

D. McAllester and K. Stratos. Formal Limitations on the Measurement of Mutual Information. In *AISTATS*, pages 875–884, 2020.

T. Mikolov, I. Sutskever, K. Chen, G. Corrado, and J. Dean. Distributed Representations of Words and Phrases and their Compositionality. In *NeurIPS*, pages 3111–3119, 2013.

T. Mikolov, E. Grave, P. Bojanowski, C. Puhrsch, and A. Joulin. Advances in Pre-Training Distributed Word Representations. In *LREC*, pages 52–55, 2018.

J. Mitrovic, B. McWilliams, J. Walker, L. Buesing, and C. Blundell. Representation Learning via Invariant Causal Mechanisms. In *ICLR*, 2021.

T. Nakata and I. Kubo. A Coupon Collector's Problem with Bonuses. In *Fourth Colloquium on Mathematics and Computer Science*, pages 215–224, 2006.

A. Newell and J. Deng. How Useful is Self-Supervised Pretraining for Visual Tasks? In *CVPR*, pages 7345–7354, 2020.

M. Noroozi and P. Favaro. Unsupervised Learning of Visual Representations by Solving Jigsaw Puzzles. In *ECCV*, pages 69–84, 2016.

K. Nozawa, P. Germain, and B. Guedj. PAC-Bayesian Contrastive Unsupervised Representation Learning. In *UAI*, pages 21–30, 2020.

A. Paszke, S. Gross, F. Massa, A. Lerer, J. Bradbury, G. Chanan, T. Killeen, Z. Lin, N. Gimelshein, L. Antiga, A. Desmaison, A. Köpf, E. Yang, Z. DeVito, M. Raison, A. Tejani, S. Chilamkurthy, B. Steiner, L. Fang, J. Bai, and S. Chintala. PyTorch: An Imperative Style, High-Performance Deep Learning Library. In *NeurIPS*, pages 8024–8035, 2019.

D. Pathak, P. Krähenbühl, J. Donahue, T. Darrell, and A. A. Efros. Context Encoders: Feature Learning by Inpainting. In *CVPR*, pages 2536–2544, 2016.

F. Pedregosa, G. Varoquaux, A. Gramfort, V. Michel, B. Thirion, O. Grisel, M. Blondel, P. Prettenhofer, R. Weiss, V. Dubourg, J. Vanderplas, A. Passos, D. Cournapeau, M. Brucher, M. Perrot, and Édouard Duchesnay. Scikit-learn: Machine Learning in Python. *Journal of Machine Learning Research*, 12(85):2825–2830, 2011.

J. Reback, W. McKinney, jbrockmendel, J. V. den Bossche, T. Augspurger, P. Cloud, gfyoung, Sinhrks, A. Klein, M. Roeschke, S. Hawkins, J. Tratner, C. She, W. Ayd, T. Petersen, M. Garcia, J. Schendel, A. Hayden, MomIsBestFriend, V. Jancauskas, P. Battiston, S. Seabold, chris-b1, h-vetinari, S. Hoyer, W. Overmeire, alimcmaster1, K. Dong, C. Whelan, and M. Mehyar. pandas-dev/pandas: Pandas 1.0.3, Mar. 2020. URL `https://doi.org/10.5281/zenodo.3715232`.

N. Saunshi, S. Malladi, and S. Arora. A Mathematical Exploration of Why Language Models Help Solve Downstream Tasks. In *ICLR*, 2021.

L. Schmarje, M. Santarossa, S.-M. Schröder, and R. Koch. A Survey on Semi-, Self-and Unsupervised Learning in Image Classification. *IEEE Access*, 9:82146–82168, 2021.

J. Snell, K. S. Twitter, and R. S. Zemel. Prototypical Networks for Few-shot Learning. In *NeurIPS*, pages 4077–4087, 2017.

I. Sutskever, J. Martens, G. Dahl, and G. Hinton. On the Importance of Initialization and Momentum in Deep Learning. In *ICML*, pages 1139–1147, 2013.

O. Tange. GNU Parallel, Nov. 2020. URL `https://doi.org/10.5281/zenodo.4284075`.

Y. Tian, X. Chen, and S. Ganguli. Understanding Self-Supervised Learning Dynamics without Contrastive Pairs. In *ICML*, pages 10268–10278, 2021.

M. K. Titsias. One-vs-Each Approximation to Softmax for Scalable Estimation of Probabilities. In *NeurIPS*, pages 4168–4176, 2016.

C. Tosh, A. Krishnamurthy, and D. Hsu. Contrastive Learning, Multi-view Redundancy, and Linear Models. In *ALT*, pages 1179–1206, 2021.

M. Tschannen, J. Djolonga, P. K. Rubenstein, S. Gelly, and M. Lucic. On Mutual Information Maximization for Representation Learning. In *ICLR*, 2020.

A. van den Oord, Y. Li, and O. Vinyals. Representation Learning with Contrastive Predictive Coding. *arXiv:1807.03748v2 [cs.LG]*, 2018.

P. Vincent, H. Larochelle, Y. Bengio, and P.-A. Manzagol. Extracting and Composing Robust Features with Denoising Autoencoders. In *ICML*, pages 1096–1103, 2008.

P. Virtanen, R. Gommers, T. E. Oliphant, M. Haberland, T. Reddy, D. Cournapeau, E. Burovski, P. Peterson, W. Weckesser, J. Bright, S. J. van der Walt, M. Brett, J. Wilson, K. J. Millman, N. Mayorov, A. R. J. Nelson, E. Jones, R. Kern, E. Larson, C. J. Carey, İ. Polat, Y. Feng, E. W. Moore, J. VanderPlas, D. Laxalde, J. Perktold, R. Cimrman, I. Henriksen, E. A. Quintero, C. R. Harris, A. M. Archibald, A. H. Ribeiro, F. Pedregosa, P. van Mulbregt, and SciPy 1.0 Contributors. SciPy 1.0: Fundamental Algorithms for Scientific Computing in Python. *Nature Methods*, 17:261–272, 2020. doi: 10.1038/s41592-019-0686-2.

T. Wang and P. Isola. Understanding Contrastive Representation Learning through Alignment and Uniformity on the Hypersphere. In *ICML*, pages 9929–9939, 2020.

W. Y. Wang and D. Yang. That's So Annoying!!!: A Lexical and Frame-Semantic Embedding Based Data Augmentation Approach to Automatic Categorization of Annoying Behaviors using #petpeeve Tweets. In *EMNLP*, pages 2557–2563, 2015.

M. L. Waskom. seaborn: Statistical Data Visualization. *Journal of Open Source Software*, 6(60):3021, 2021. doi: 10.21105/joss.03021. URL `https://doi.org/10.21105/joss.03021`.

C. Wei, K. Shen, Y. Chen, and T. Ma. Theoretical Analysis of Self-Training with Deep Networks on Unlabeled Data. In *ICLR*, 2021.

Z. Wu, Y. Xiong, S. X. Yu, and D. Lin. Unsupervised Feature Learning via Non-Parametric Instance Discrimination. In *CVPR*, pages 3733–3742, 2018.

O. Yadan. Hydra - A Framework for Elegantly Configuring Complex Applications. GitHub, 2019. URL `https://github.com/facebookresearch/hydra`.

Y. You, I. Gitman, and B. Ginsburg. Large Batch Training of Convolutional Networks. *arXiv:1708.03888v3 [cs.CV]*, 2017.

R. Zhang, P. Isola, and A. A. Efros. Colorful Image Colorization. In *ECCV*, pages 649–666, 2016.

R. Zhang, P. Isola, and A. A. Efros. Split-Brain Autoencoders: Unsupervised Learning by Cross-Channel Prediction. In *CVPR*, pages 1058–1067, 2017.

X. Zhang, J. Zhao, and Y. LeCun. Character-level Convolutional Networks for Text Classification. In *NeurIPS*, pages 649–657, 2015.

A Notations

Table 2 summarizes our notations.

B Relationship between Latent Classes and Supervised classes

In the main body of the manuscript, we assume that the latent classes C are a superset of the supervised classes Y. Here, we mention a few scenarios covered by our analysis.

Supervised Class is a Union of Latent Classes Suppose that latent classes C are breeds of dog and cat for image classification and supervised class $y \in \mathsf{Y}$ is a union of breeds: "dog" or "cat". In this setting, the downstream classifier can mispredict the class label among dog breeds for a dog image. Therefore the classifier's loss on all latent classes $\mathsf{Y} = \mathsf{C}$ is higher than or equal to the same classifier' loss on the union set at worst.

Supervised Class is a Product of Latent Classes Another practical scenario is that the supervised class is a product of latent classes. Suppose that the latent classes are disentangled properties of dog/cat, such as breeds and color. In this case, a sample can be drawn from different latent classes, for example, a white golden retriever image can be drawn from "Golden Retriever" class and "white" class. Suppose that we perform classification over the product of the latent classes such as "White Golden Retriever" and "Black Ragamuffin" at the supervised step. Since we use Jensen's inequality to aggregate feature representation into the weights of mean classifier in Section 3.2, our analysis can deal with this case as well.

C Relation of Mean Classifier and Linear Classifier

Recall that $\mathbf{g} : \mathsf{R}^h \to \mathsf{R}^Y$ that is a function from a feature space to a label space. Suppose $\widehat{\mathbf{g}} = \operatorname{argmin}_{\mathbf{g}} L_{\mathsf{sup}}(\mathbf{g} \circ \mathbf{f})$. The mean classifier's supervised loss is bounded by a loss with $\widehat{\mathbf{g}}$:

$$L^{\mu}_{\mathsf{sup}}(\mathbf{f}) \leq L_{\mathsf{sup}}(\widehat{\mathbf{g}} \circ \mathbf{f}). \tag{12}$$

This relation holds with sub-class loss in Definition 4 as well.

Note that the mean classifier is a special case of the linear classifier [Snell et al., 2017, Sec. 2.4]. A linear classifier is defined as $\mathbf{W}\mathbf{f}(\mathbf{a}(\mathbf{x})) + \mathbf{b}$, where $\mathbf{W} \in \mathsf{R}^{Y \times h}$ and $\mathbf{b} \in \mathsf{R}^Y$. When $\mathbf{W} = [\boldsymbol{\mu}_1, \ldots, \boldsymbol{\mu}_Y]^\top$ and $\mathbf{b} = \mathbf{0}$, the linear classifier is equivalent to the mean classifier.

D Proofs

D.1 Inequality for Eq. (7)

We show the following inequality used to obtain Eq. (7):

$$\begin{aligned}
&\mathop{\mathsf{E}}_{c, f_{c_k} g_{k=1}^K \rho^{K+1}} \mathop{\mathsf{E}}_{\substack{\mathbf{x} \\ \mathbf{a}}} \mathop{\mathsf{E}}_{\substack{D_c \\ A}} \ell_{\mathsf{Info}}\left(\mathbf{z}, \left\{\boldsymbol{\mu}(\mathbf{x}), \boldsymbol{\mu}_{c_1}, \ldots, \boldsymbol{\mu}_{c_K}\right\}\right) \\
&\mathop{\mathsf{E}}_{c, f_{c_k} g_{k=1}^K \rho^{K+1}} \mathop{\mathsf{E}}_{\substack{\mathbf{x} \\ \mathbf{a}}} \mathop{\mathsf{E}}_{\substack{D_c \\ A}} \ell_{\mathsf{Info}}\left(\mathbf{z}, \left\{\boldsymbol{\mu}_c, \boldsymbol{\mu}_{c_1}, \ldots, \boldsymbol{\mu}_{c_K}\right\}\right) + d(\mathbf{f}).
\end{aligned} \tag{13}$$

Table 2: Notations

Symbol	Description
c	Latent class
c	Latent class of a negative sample
h	The dimensionality of feature representation $\mathbf{z}$
t	Temperature parameter in InfoNCE loss (1)
y	Supervised class
K	The number of negative samples
N	The number of samples used in self-supervised learning
N_y	The number of samples whose label is y
Y	The number of supervised classes
α	Non-negative coefficient in Eq. (11)
β	Non-negative coefficient in Eq. (11)
τ	Collision probability in Proposition 6
υ	Probability to draw all latent class defined in Section 4.1
C	Latent classes associated with Y
$\mathsf{C}_{\mathsf{sub}}$	Function to remove duplicated latent classes
X	Input space
Y	Supervised class space
$\mathsf{Y}_{\mathsf{sub}}$	Subset of Y
A	Distribution of data augmentations
D_y	Distribution over X conditioned on supervised class y
D_c	Distribution over X conditioned on latent class c
S	Joint distribution over X Y
$\mathsf{S}_{\mathsf{sub}}$	Joint distribution over X $\mathsf{Y}_{\mathsf{sub}}$
ρ	Probability distribution over C
$\mathbf{a}$	Data augmentation: X ! X
$\mathbf{a}^+$	Data augmentation to create positive feature representation
$\mathbf{a}^-$	Data augmentation to create negative feature representation
$\mathbf{f}$	Feature extractor: X ! R^h
$\widehat{\mathbf{f}}$	Trained feature extractor by minimizing $\widehat{L}_{\mathsf{Info}}$
$\mathbf{g}$	Supervised classifier taken a feature representation $\mathbf{z}$: R^h ! R^Y
$\mathbf{q}$	Function that outputs real-valued vector used in Proposition 10
$\mathbf{x}$	Input sample in X
$\mathbf{z}$	L2 normalized feature representation: $\mathbf{f}(\mathbf{a}(\mathbf{x}))$
$\mathbf{z}^+$	Positive L2 normalized feature representation: $\mathbf{f}(\mathbf{a}^+(\mathbf{x}))$
$\mathbf{z}^-$	Negative L2 normalized feature representation: $\mathbf{f}(\mathbf{a}^-(\mathbf{x}^-))$
$\mathbf{Z}$	Set of positive and K negative features: $\{\mathbf{z}^+, \mathbf{z}_1^-, \ldots, \mathbf{z}_K^-\}$
$\boldsymbol{\mu}(\mathbf{x})$	Averaged feature representation over A: $\mathsf{E}_{\mathbf{a}\ \mathsf{A}}\, \mathbf{f}(\mathbf{a}(\mathbf{x}))$
$\boldsymbol{\mu}_c$	Mean classifier's weight vector of latent class c: $\mathsf{E}_{\mathbf{x}\ \mathsf{D}_c}\, \boldsymbol{\mu}(\mathbf{x})$
$\boldsymbol{\mu}_y$	Mean classifier's weight vector of supervised class y: $\mathsf{E}_{\mathbf{x}\ \mathsf{D}_y}\, \boldsymbol{\mu}(\mathbf{x})$
$\mathrm{Col}(\ ,\ )$	Collision value defined in Section 3.2: $\sum_{k=1}^{K} \mathsf{I}[c^k = c_k^-]$
$d(\ )$	Gap term defined in Eq. (7)
ℓ_{Info}	InfoNCE-based self-supervised loss defined by Eq. (1)
$\ell_{\mathsf{sub}}^{\mu}$	Mean classifier's supervised sub-class loss defined by Eq. (16)
L_{Info}	Expected self-supervised loss defined by Eq. (2)
$\widehat{L}_{\mathsf{Info}}$	Empirical self-supervised loss
L_{sup}	Supervised loss defined by Eq. (3)
L_{sub}	Supervised sub-class loss defined by Eq. (5)
L_{sup}^{μ}	Supervised loss of mean classifier defined by Eq. (4)
L_{sub}^{μ}	Sub-class supervised loss of mean classifier by Eq. (6)
$\mathsf{I}[\ ]$	Indicator function
$(.\ .)$	Inner product

Proof. We replace $\boldsymbol{\mu}(\mathbf{x})$ with $\boldsymbol{\mu}_c$ in the left hand side of Eq. (13):

$$
\begin{aligned}
&\mathop{\mathsf{E}}_{c, f c_k g_{k=1}^K \quad \rho^{K+1}} \quad \mathop{\mathsf{E}}_{\substack{\mathbf{x} \quad D_c \\ \mathbf{a} \quad A}} \ell_{\mathsf{Info}}\left(\mathbf{z}, \left\{\boldsymbol{\mu}(\mathbf{x}), \boldsymbol{\mu}_{c_1}, \ldots, \boldsymbol{\mu}_{c_K}\right\}\right) \\
= &\mathop{\mathsf{E}}_{c, f c_k g_{k=1}^K \quad \rho^{K+1}} \quad \mathop{\mathsf{E}}_{\substack{\mathbf{x} \quad D_c \\ \mathbf{a} \quad A}} \ell_{\mathsf{Info}}\left(\mathbf{z}, \left\{\boldsymbol{\mu}(\mathbf{x}), \boldsymbol{\mu}_{c_1}, \ldots, \boldsymbol{\mu}_{c_K}\right\}\right) \\
&+ \mathop{\mathsf{E}}_{c, f c_k g_{k=1}^K \quad \rho^{K+1}} \quad \mathop{\mathsf{E}}_{\substack{\mathbf{x} \quad D_c \\ \mathbf{a} \quad A}} \ell_{\mathsf{Info}}\left(\mathbf{z}, \left\{\boldsymbol{\mu}_c, \boldsymbol{\mu}_{c_1}, \ldots, \boldsymbol{\mu}_{c_K}\right\}\right) \\
&\quad \mathop{\mathsf{E}}_{c, f c_k g_{k=1}^K \quad \rho^{K+1}} \quad \mathop{\mathsf{E}}_{\substack{\mathbf{x} \quad D_c \\ \mathbf{a} \quad A}} \ell_{\mathsf{Info}}\left(\mathbf{z}, \left\{\boldsymbol{\mu}_c, \boldsymbol{\mu}_{c_1}, \ldots, \boldsymbol{\mu}_{c_K}\right\}\right) \\
= &\mathop{\mathsf{E}}_{c, f c_k g_{k=1}^K \quad \rho^{K+1}} \quad \mathop{\mathsf{E}}_{\substack{\mathbf{x} \quad D_c \\ \mathbf{a} \quad A}} \ell_{\mathsf{Info}}\left(\mathbf{z}, \left\{\boldsymbol{\mu}_c, \boldsymbol{\mu}_{c_1}, \ldots, \boldsymbol{\mu}_{c_K}\right\}\right) \\
&+ \underbrace{\mathop{\mathsf{E}}_{c, f c_k g_{k=1}^K \quad \rho^{K+1}} \quad \mathop{\mathsf{E}}_{\substack{\mathbf{x} \quad D_c \\ \mathbf{a} \quad A}} \left[\ell_{\mathsf{Info}}\left(\mathbf{z}, \left\{\boldsymbol{\mu}(\mathbf{x}), \boldsymbol{\mu}_{c_1}, \ldots, \boldsymbol{\mu}_{c_K}\right\}\right) \quad \ell_{\mathsf{Info}}\left(\mathbf{z}, \left\{\boldsymbol{\mu}_c, \boldsymbol{\mu}_{c_1}, \ldots, \boldsymbol{\mu}_{c_K}\right\}\right)\right]}_{\text{Gap term}}.
\end{aligned}
\tag{14}
$$

When the gap term is non-negative: $\mathbf{z} \quad \boldsymbol{\mu}(\mathbf{x}) \quad \mathbf{z} \quad \boldsymbol{\mu}_c$, we drop it from Eq. (14) to obtain the lower bound (13) with $d(\mathbf{f}) = 0$. Thus we consider a lower bound of the gap term when the gap term is negative, $\mathbf{z} \quad \boldsymbol{\mu}(\mathbf{x}) > \mathbf{z} \quad \boldsymbol{\mu}_c$, to guarantee Eq. (14). As a general case, we show the bound with temperature parameter t.

The gap term in Eq. (14)

$$
\begin{aligned}
&= \mathop{\mathsf{E}}_{c, f c_k g_{k=1}^K \quad \rho^{K+1}} \quad \mathop{\mathsf{E}}_{\substack{\mathbf{x} \quad D_c \\ \mathbf{a} \quad A}} [\mathbf{z} \quad (\boldsymbol{\mu}_c \quad \boldsymbol{\mu}(\mathbf{x}))/t] + \underbrace{\ln \frac{\exp\left(\mathbf{z} \quad \boldsymbol{\mu}(\mathbf{x})/t\right) + \sum_{k=1}^K \exp\left(\mathbf{z} \quad \boldsymbol{\mu}_{c_k}/t\right)}{\exp(\mathbf{z} \quad \boldsymbol{\mu}_c/t) + \sum_{k=1}^K \exp\left(\mathbf{z} \quad \boldsymbol{\mu}_{c_k}/t\right)}}_{\text{Non-negative}} \\
&> \frac{1}{t} \mathop{\mathsf{E}}_{c \quad \rho} \mathop{\mathsf{E}}_{\substack{\mathbf{x} \quad D_c \\ \mathbf{a} \quad A}} [\mathbf{z} \quad (\boldsymbol{\mu}_c \quad \boldsymbol{\mu}(\mathbf{x}))] \\
&= \frac{1}{t} \mathop{\mathsf{E}}_{c \quad \rho} \mathop{\mathsf{E}}_{\mathbf{x} \quad D_c} \left[\mathop{\mathsf{E}}_{\mathbf{a} \quad A} [\mathbf{f}(\mathbf{a}(\mathbf{x}))] \quad \left(\mathop{\mathsf{E}}_{\substack{\mathbf{x}^+ \quad D_c \\ \mathbf{a}_1^+ \quad A}} \left[\mathbf{f}(\mathbf{a}_1^+(\mathbf{x}^+))\right] \quad \mathop{\mathsf{E}}_{\mathbf{a}_2^+ \quad A} \left[\mathbf{f}(\mathbf{a}_2^+(\mathbf{x}))\right]\right)\right] \qquad (15) \\
&:= d(\mathbf{f}).
\end{aligned}
$$

□

D.2 Proof of Proposition 6

Proposition 6 (CURL Lower Bound of Self-supervised Loss)**.** *For all feature extractor* $\mathbf{f}$,

$$
\begin{aligned}
L_{\mathsf{Info}}(\mathbf{f}) \quad (1 \quad \tau_K) \mathop{\mathsf{E}}_{c, f c_k g_{k=1}^K \quad \rho^{K+1}} &[\underbrace{L_{\mathsf{sub}}^{\mu}(\mathbf{f}, C_{\mathsf{sub}})}_{\textit{sub-class loss}} \; j \; \mathrm{Col} = 0] \\
+\tau_K \mathop{\mathsf{E}}_{c, f c_k g_{k=1}^K \quad \rho^{K+1}} &[\underbrace{\ln(\mathrm{Col}+1)}_{\textit{collision}} \; j \; \mathrm{Col} \neq 0] + d(\mathbf{f}).
\end{aligned}
\tag{8}
$$

We apply the proof of Theorem B.1 in Arora et al. [2019] to the self-supervised learning setting.

Proof. Before showing the inequality, we define the following sub-class loss with mean classifier for single $\mathbf{z}$ with c and $C_{\mathsf{sub}}(f c, c_1, \ldots, c_K g)$:

$$
\ell_{\mathsf{sub}}^{\mu}(\mathbf{z}, c, C_{\mathsf{sub}}) := \quad \ln \frac{\exp\left(\mathbf{z} \quad \boldsymbol{\mu}_c\right)}{\sum_{j 2 C_{\mathsf{sub}}} \exp\left(\mathbf{z} \quad \boldsymbol{\mu}_j\right)}. \tag{16}
$$

We start from Eq. (7).

$$
\begin{aligned}
(7) = (1 \quad \tau_K) & \mathop{\mathbb{E}}_{c, \{c_k\}_{k=1}^K \quad \rho^{K+1}} \quad \mathop{\mathbb{E}}_{\substack{\mathbf{x} \quad D_c \\ \mathbf{a} \quad A}} \left[\ell_{\mathsf{Info}} \left(\mathbf{z}, \left\{ \boldsymbol{\mu}_c, \boldsymbol{\mu}_{c_1}, \dots, \boldsymbol{\mu}_{c_K} \right\} \right) \mid \mathrm{Col}\left(c, \{c_k\}_{k=1}^K\right) = 0 \right] \\
& + \tau_K \mathop{\mathbb{E}}_{c, \{c_k\}_{k=1}^K \quad \rho^{K+1}} \quad \mathop{\mathbb{E}}_{\substack{\mathbf{x} \quad D_c \\ \mathbf{a} \quad A}} \left[\ell_{\mathsf{Info}} \left(\mathbf{z}, \left\{ \boldsymbol{\mu}_c, \boldsymbol{\mu}_{c_1}, \dots, \boldsymbol{\mu}_{c_K} \right\} \right) \mid \mathrm{Col}\left(c, \{c_k\}_{k=1}^K\right) \neq 0 \right] + d(\mathbf{f}) \\
(1 \quad \tau_K) & \mathop{\mathbb{E}}_{c, \{c_k\}_{k=1}^K \quad \rho^{K+1}} \quad \mathop{\mathbb{E}}_{\substack{\mathbf{x} \quad D_c \\ \mathbf{a} \quad A}} \left[\ell^{\mu}_{\mathsf{sub}}(\mathbf{z}, c, \mathsf{C}_{\mathsf{sub}}) \mid \mathrm{Col} = 0 \right] \\
& + \tau_K \mathop{\mathbb{E}}_{c, \{c_k\}_{k=1}^K \quad \rho^{K+1}} \quad \mathop{\mathbb{E}}_{\substack{\mathbf{x} \quad D_c \\ \mathbf{a} \quad A}} \left[\ell^{\mu}_{\mathsf{sub}}(\mathbf{z}, c, \{c\}^{\mathrm{Col}+1}) \mid \mathrm{Col} \neq 0 \right] + d(\mathbf{f}) \\
= (1 \quad \tau_K) & \mathop{\mathbb{E}}_{c, \{c_k\}_{k=1}^K \quad \rho^{K+1}} \quad \left[L^{\mu}_{\mathsf{sub}}(\mathbf{z}, \mathsf{C}_{\mathsf{sub}}) \mid \mathrm{Col} = 0 \right] \\
& + \tau_K \mathop{\mathbb{E}}_{c, \{c_k\}_{k=1}^K \quad \rho^{K+1}} \quad \left[\ln(\mathrm{Col}+1) \mid \mathrm{Col} \neq 0 \right] + d(\mathbf{f}), \qquad (17)
\end{aligned}
$$

where $\{c\}^{\mathrm{Col}+1}$ is a bag of latent classes that contains only c and the number of c is $\mathrm{Col}(c, \{c_k\}_{k=1}^K)+1$.

The first equation is done by using collision probability τ_K conditioned on Col. The inequality is obtained by removing duplicated latent classes from the first term and removing the other latent classes from the second term. Note that InfoNCE is a monotonically increasing function; its value decreases by removing any elements in the negative features in the loss. □

D.3 Proof of Theorem 8

Theorem 8 (Proposed Lower Bound of Self-supervised Loss)**.** *For all feature extractor* $\mathbf{f}$*,*

$$
\begin{aligned}
L_{\mathsf{Info}}(\mathbf{f}) \quad \frac{1}{2} \Big\{ & \upsilon_{K+1} \mathop{\mathbb{E}}_{c, \{c_k\}_{k=1}^K \quad \rho^{K+1}} \left[\underbrace{L^{\mu}_{\mathsf{sub}}(\mathbf{f}, \mathsf{C})}_{\textit{sup. loss}} \mid \mathsf{C}_{\mathsf{sub}} = \mathsf{C} \right] \\
& + (1 \quad \upsilon_{K+1}) \mathop{\mathbb{E}}_{c, \{c_k\}_{k=1}^K \quad \rho^{K+1}} \left[\underbrace{L^{\mu}_{\mathsf{sub}}(\mathbf{f}, \mathsf{C}_{\mathsf{sub}})}_{\textit{sub-class loss}} \mid \mathsf{C}_{\mathsf{sub}} \neq \mathsf{C} \right] \\
& + \mathop{\mathbb{E}}_{c, \{c_k\}_{k=1}^K \quad \rho^{K+1}} \underbrace{\ln(\mathrm{Col}+1)}_{\textit{collision}} \Big\} + d(\mathbf{f}). \qquad (10)
\end{aligned}
$$

Proof. We start from Eq. (7).

$$
\begin{aligned}
(7) = \quad & \upsilon_{K+1} \mathop{\mathbb{E}}_{c, \{c_k\}_{k=1}^K \quad \rho^{K+1}} \mathop{\mathbb{E}}_{\substack{\mathbf{x} \quad D_c \\ \mathbf{a} \quad A}} \left[\ell_{\mathsf{Info}} \left(\mathbf{z}, \left\{ \boldsymbol{\mu}_c, \boldsymbol{\mu}_{c_1}, \dots, \boldsymbol{\mu}_{c_K} \right\} \right) \mid \mathsf{C}_{\mathsf{sub}}(\{c, c_1, \dots, c_K\}) = \mathsf{C} \right] \\
& + (1 \quad \upsilon_{K+1}) \mathop{\mathbb{E}}_{c, \{c_k\}_{k=1}^K \quad \rho^{K+1}} \mathop{\mathbb{E}}_{\substack{\mathbf{x} \quad D_c \\ \mathbf{a} \quad A}} \left[\ell_{\mathsf{Info}} \left(\mathbf{z}, \left\{ \boldsymbol{\mu}_c, \boldsymbol{\mu}_{c_1}, \dots, \boldsymbol{\mu}_{c_K} \right\} \right) \mid \mathsf{C}_{\mathsf{sub}}(\{c, c_1, \dots, c_K\}) \neq \mathsf{C} \right] + d(\mathbf{f}) \qquad (18) \\
& \frac{1}{2} \Big\{ \upsilon_{K+1} \mathop{\mathbb{E}}_{c, \{c_k\}_{k=1}^K \quad \rho^{K+1}} \mathop{\mathbb{E}}_{\substack{\mathbf{x} \quad D_c \\ \mathbf{a} \quad A}} \left[\ell^{\mu}_{\mathsf{sub}}(\mathbf{z}, c, \mathsf{C}_{\mathsf{sub}}) \mid \mathsf{C}_{\mathsf{sub}} = \mathsf{C} \right] \\
& + (1 \quad \upsilon_{K+1}) \mathop{\mathbb{E}}_{c, \{c_k\}_{k=1}^K \quad \rho^{K+1}} \mathop{\mathbb{E}}_{\substack{\mathbf{x} \quad D_c \\ \mathbf{a} \quad A}} \left[\ell^{\mu}_{\mathsf{sub}}(\mathbf{z}, c, \mathsf{C}_{\mathsf{sub}}) \mid \mathsf{C}_{\mathsf{sub}} \neq \mathsf{C} \right] \\
& + \mathop{\mathbb{E}}_{c, \{c_k\}_{k=1}^K \quad \rho^{K+1}} \ln\left(\mathrm{Col}\left(c, \{c_k\}_{k=1}^K\right) + 1\right) \Big\} + d(\mathbf{f}), \qquad (19)
\end{aligned}
$$

where recall that $\ell^{\mu}_{\mathsf{sub}}$ is defined by Eq. (16).

The first equation is obtained by using the definition of υ to distinguish whether or not the sampled latent classes contain all latent classes C. To derive the inequality, we use the following properties of

the cross-entropy loss. Fixed $\mathbf{f}$ and c, for all K $\{1, \ldots, K\}$, the value of ℓ_{Info} holds the following inequality:

$$\ell_{\mathsf{Info}}\left(\mathbf{z}, \left\{\boldsymbol{\mu}_c \cup \{\boldsymbol{\mu}_{c_k}\}_{k=1}^{K}\right\}\right) \quad \ell_{\mathsf{Info}}\left(\mathbf{z}, \{\boldsymbol{\mu}_c \cup \{\boldsymbol{\mu}_{c_k}\}_{k2K}\right). \tag{20}$$

Thus we apply the following inequalities to the first and second terms in Eq. (18).

$$\begin{aligned}\ell_{\mathsf{Info}}\left(\mathbf{z}, \left\{\boldsymbol{\mu}_c, \boldsymbol{\mu}_{c_1}, \ldots, \boldsymbol{\mu}_{c_K}\right\}\right) \quad & \frac{1}{2}\left[\ell^{\mu}_{\mathsf{sub}}\left(\mathbf{z}, c, \mathsf{C}_{\mathsf{sub}}\right) + \ell^{\mu}_{\mathsf{sub}}\left(\mathbf{z}, c, \{c\} \cup \mathsf{Col}+1\right)\right] \\ & = \frac{1}{2}\left[\ell^{\mu}_{\mathsf{sub}}\left(\mathbf{z}, c, \mathsf{C}_{\mathsf{sub}}\right) + \ln(\mathrm{Col}+1)\right]\end{aligned} \tag{21}$$

By following the notations of L^{μ}_{sup} and L^{μ}_{sub}, we obtain the lower bound (10) in Theorem 8 from Eq. (19). □

D.4 Proof of Corollary 9

Corollary 9 (Upper Bound of Collision Term)**.** *Given a latent class c, K negative classes $\{c_k\}_{k=1}^{K}$, and feature extractor $\mathbf{f}$,*

$$\ln\left(\mathrm{Col}\left(c, \{c_k\}_{k=1}^{K}\right)+1\right) \quad \alpha + \beta \mathop{\mathbb{E}}_{\substack{\mathbf{x} \sim D_c \\ (\mathbf{a}, \mathbf{a}^+) \sim A^2}} \mathop{\mathbb{E}}_{\mathbf{x}^0 \sim D_c} \left|\mathbf{f}(\mathbf{a}(\mathbf{x})) \quad \left[\mathbf{f}(\mathbf{a}^0(\mathbf{x}^0)) \quad \mathbf{f}(\mathbf{a}^+(\mathbf{x}))\right]\right|, \tag{11}$$

where α and β are non-negative constants depending on the number of duplicated latent classes.

We prove Corollary 9 that shows the upper bound of the collision term to understand the effect of the number of negative samples. Our proof is inspired by Arora et al. [2019, Lemma A.1]. As a general case, we consider the loss function with temperature parameter t.

Proof. We decompose the self-supervised loss L_{Info} by using υ to extract the collision term.

$$\begin{aligned}
& L_{\mathsf{Info}}(\mathbf{f}) \\
& = \upsilon_{K+1} \left[\mathop{\mathbb{E}}_{c, \{c_k\}_{k=1}^{K} \sim \rho^{K+1}} \mathop{\mathbb{E}}_{\substack{\mathbf{x} \sim D_c \\ (\mathbf{a}, \mathbf{a}^+) \sim A^2}} \mathop{\mathbb{E}}_{\substack{\{\mathbf{x}_k\}_{k=1}^{K} \sim \{D_{c_k}\}_{k=1}^{K} \\ \{\mathbf{a}_k\}_{k=1}^{K} \sim \{A\}^K}} \left[\ell_{\mathsf{Info}}(\mathbf{z}, \mathbf{Z}) \mid \mathsf{C}_{\mathsf{sub}}(\{c, c_1, \ldots, c_K\}) = \mathsf{C}\right] \right] \\
& \quad + (1 \quad \upsilon_{K+1}) \left[\mathop{\mathbb{E}}_{c, \{c_k\}_{k=1}^{K} \sim \rho^{K+1}} \mathop{\mathbb{E}}_{\substack{\mathbf{x} \sim D_c \\ (\mathbf{a}, \mathbf{a}^+) \sim A^2}} \mathop{\mathbb{E}}_{\substack{\{\mathbf{x}_k\}_{k=1}^{K} \sim \{D_{c_k}\}_{k=1}^{K} \\ \{\mathbf{a}_k\}_{k=1}^{K} \sim \{A\}^K}} \left[\ell_{\mathsf{Info}}(\mathbf{z}, \mathbf{Z}) \mid \mathsf{C}_{\mathsf{sub}}(\{c, c_1, \ldots, c_K\}) \neq \mathsf{C}\right] \right] \\
& \quad \upsilon_{K+1} \left[\mathop{\mathbb{E}}_{c, \{c_k\}_{k=1}^{K} \sim \rho^{K+1}} \mathop{\mathbb{E}}_{\substack{\mathbf{x} \sim D_c \\ (\mathbf{a}, \mathbf{a}^+) \sim A^2}} \mathop{\mathbb{E}}_{\substack{\{\mathbf{x}_k\}_{k=1}^{K} \sim \{D_{c_k}\}_{k=1}^{K} \\ \{\mathbf{a}_k\}_{k=1}^{K} \sim \{A\}^K}} \left[\ell_{\mathsf{Info}}\left(\mathbf{z}, \{\mathbf{z}_k\}_{c \neq c_k}\right) + \ell_{\mathsf{Info}}\left(\mathbf{z}, \{\mathbf{z}_k\}_{c=c_k}\right) \mid \mathsf{C}_{\mathsf{sub}} = \mathsf{C}\right] \right] \\
& \quad + (1 \quad \upsilon_{K+1}) \left[\mathop{\mathbb{E}}_{c, \{c_k\}_{k=1}^{K} \sim \rho^{K+1}} \mathop{\mathbb{E}}_{\substack{\mathbf{x} \sim D_c \\ (\mathbf{a}, \mathbf{a}^+) \sim A^2}} \mathop{\mathbb{E}}_{\substack{\{\mathbf{x}_k\}_{k=1}^{K} \sim \{D_{c_k}\}_{k=1}^{K} \\ \{\mathbf{a}_k\}_{k=1}^{K} \sim \{A\}^K}} \left[\ell_{\mathsf{Info}}\left(\mathbf{z}, \{\mathbf{z}_k\}_{c \neq c_k}\right) + \ell_{\mathsf{Info}}\left(\mathbf{z}, \{\mathbf{z}_k\}_{c=c_k}\right) \mid \mathsf{C}_{\mathsf{sub}} \neq \mathsf{C}\right] \right] \\
& = \mathop{\mathbb{E}}_{c, \{c_k\}_{k=1}^{K} \sim \rho^{K+1}} \mathop{\mathbb{E}}_{\substack{\mathbf{x} \sim D_c \\ (\mathbf{a}, \mathbf{a}^+) \sim A^2}} \mathop{\mathbb{E}}_{\substack{\{\mathbf{x}_k\}_{k=1}^{K} \sim \{D_{c_k}\}_{k=1}^{K} \\ \{\mathbf{a}_k\}_{k=1}^{K} \sim \{A\}^K}} \ell_{\mathsf{Info}}\left(\mathbf{z}, \{\mathbf{z}_k\}_{c=c_k}\right) + \mathrm{Reminder} \\
& = \mathop{\mathbb{E}}_{c} \mathop{\mathbb{E}}_{\rho \mathsf{Col}} \mathop{\mathbb{E}}_{B_c} \mathop{\mathbb{E}}_{\substack{\mathbf{x}, \{\mathbf{x}_k\}_{k=1}^{\mathsf{Col}} \sim D_c^{\mathsf{Col}+1} \\ (\mathbf{a}, \mathbf{a}^+, \{\mathbf{a}_k\}_{k=1}^{\mathsf{Col}}) \sim A^{\mathsf{Col}+2}}} \ell_{\mathsf{Info}}(\mathbf{z}, \mathbf{Z}) + \mathrm{Reminder},
\end{aligned} \tag{22}$$

where B_c is the probability distribution over Col conditioned on c with K. The first equality is done by decomposition with v. The inequality is obtained by using the following property of the cross-entropy loss. Given K $f1, \ldots, Kg$,

$$\ell_{\mathsf{Info}}(\mathbf{z}, \mathbf{Z}) \quad \ell_{\mathsf{Info}}\left(\mathbf{z}, f\mathbf{z}^{+}g \left[f\mathbf{z}_k g_{k2K}\right) + \ell_{\mathsf{Info}}\left(\mathbf{z}, f\mathbf{z}^{+}g \left[f\mathbf{z}_k g_{k2f1,\ldots,Kgnk}\right)\right.\right. . \tag{23}$$

We focus on the first term in Eq. (22), where the loss takes samples are drawn from the same latent class c. Fixed $\mathbf{f}$ and c, let $m = \max_{\mathbf{z}_k 2 \mathbf{Z}} \mathbf{z} \ \mathbf{z}_k/t$ and $\mathbf{z} \ = \operatorname{argmax}_{\mathbf{z}_k 2 \mathbf{Z}} \mathbf{z} \ \mathbf{z}_k$.

$$\begin{aligned}
&\mathop{\mathsf{E}}_{\substack{c \\ \mathsf{Col}}} \mathop{\mathsf{E}}_{\substack{\rho \\ B_c}} \mathop{\mathsf{E}}_{\substack{\mathbf{x}, f\mathbf{x}_k g_{k=1}^{\mathsf{Col}} \\ (\mathbf{a}, \mathbf{a}^{+}, f\mathbf{a}_k g_{k=1}^{\mathsf{Col}})}} \mathop{\mathsf{E}}_{\substack{D_c^{\mathsf{Col}+1} \\ A^{\mathsf{Col}+2}}} \ell_{\mathsf{Info}}(\mathbf{z}, \mathbf{Z}) \\
&\mathop{\mathsf{E}}_{\substack{c \\ \mathsf{Col}}} \mathop{\mathsf{E}}_{\substack{\rho \\ B_c}} \mathop{\mathsf{E}}_{\substack{\mathbf{x}, f\mathbf{x}_k g_{k=1}^{\mathsf{Col}} \\ (\mathbf{a}, \mathbf{a}^{+}, f\mathbf{a}_k g_{k=1}^{\mathsf{Col}})}} \mathop{\mathsf{E}}_{\substack{D_c^{\mathsf{Col}+1} \\ A^{\mathsf{Col}+2}}} \mathbf{z} \ \mathbf{z}^{+}/t + \ln\left[\exp(\mathbf{z} \ \mathbf{z}^{+}/t) + \mathrm{Col}\exp(m)\right] \\
&\mathop{\mathsf{E}}_{\substack{c \\ \mathsf{Col}}} \mathop{\mathsf{E}}_{\substack{\rho \\ B_c}} \mathop{\mathsf{E}}_{\substack{\mathbf{x}, f\mathbf{x}_k g_{k=1}^{\mathsf{Col}} \\ (\mathbf{a}, \mathbf{a}^{+}, f\mathbf{a}_k g_{k=1}^{\mathsf{Col}})}} \mathop{\mathsf{E}}_{\substack{D_c^{\mathsf{Col}+1} \\ A^{\mathsf{Col}+2}}} \max\left[\ln(\mathrm{Col}+1), \ln(\mathrm{Col}+1) \quad \mathbf{z} \ \mathbf{z}^{+}/t + m\right] \\
&\mathop{\mathsf{E}}_{\substack{c \\ \mathsf{Col}}} \mathop{\mathsf{E}}_{\substack{\rho \\ B_c}} \mathop{\mathsf{E}}_{\substack{\mathbf{x}, f\mathbf{x}_k g_{k=1}^{\mathsf{Col}} \\ (\mathbf{a}, \mathbf{a}^{+}, f\mathbf{a}_k g_{k=1}^{\mathsf{Col}})}} \mathop{\mathsf{E}}_{\substack{D_c^{\mathsf{Col}+1} \\ A^{\mathsf{Col}+2}}} \ln(\mathrm{Col}+1) + \frac{1}{t} j\mathbf{z} \ \mathbf{z} \quad \mathbf{z} \ \mathbf{z}^{+}j.
\end{aligned} \tag{24}$$

Note that $\ln(\mathrm{Col}+1)$ is the constant depending on the number of duplicated latent classes, then we focus on $j\mathbf{z} \ \mathbf{z} \quad \mathbf{z} \ \mathbf{z}^{+}j$.

$$\mathop{\mathsf{E}}_{\substack{\mathbf{x}, f\mathbf{x}_k g_{k=1}^{\mathsf{Col}} \\ (\mathbf{a}, \mathbf{a}^{+}, f\mathbf{a}_k g_{k=1}^{\mathsf{Col}})}} \mathop{\mathsf{E}}_{\substack{D_c^{\mathsf{Col}+1} \\ A^{\mathsf{Col}+2}}} j\mathbf{z} \ \mathbf{z} \quad \mathbf{z} \ \mathbf{z}^{+}j \quad (\mathrm{Col}+1) \mathop{\mathsf{E}}_{\substack{\mathbf{x} \\ (\mathbf{a}, \mathbf{a}^{+})}} \mathop{\mathsf{E}}_{\substack{D_c \\ A^2}} \mathop{\mathsf{E}}_{\substack{\mathbf{x}^{0} \\ \mathbf{a}^{0}}} \mathop{\mathsf{E}}_{\substack{D_c \\ A}} j\mathbf{z} \ \mathbf{z}^{0} \quad \mathbf{z} \ \mathbf{z}^{+}j.$$

Therefore, $\alpha = \ln(\mathrm{Col}+1)$ and $\beta = \frac{\mathsf{Col}+1}{t}$. □

D.5 Proof of Proposition 10

Proposition 10 (Optimality of L_{sub})**.** *Suppose C Y and ρ is uniform: 8c 2 C, $\rho(c) = 1/jCj$. Suppose a constant function* $\mathbf{q} : \mathbf{x}$ *2 X 7!* $\left[q_1, \ldots, q_{jCj}\right]^{>}$*. Optimal* $\mathbf{q}$ *is a constant function that outputs a vector with the same value if and only if it minimizes* $\mathsf{E}_{c, f\mathbf{c}_k g_{k=1}^{K} \ \rho^{K+1}} L_{\mathsf{sub}}(\mathbf{q} \ , C_{\mathsf{sub}})$*. The optimal* $\mathbf{q}$ *is also the minimizer of* L_{sup}*.*

Proof. Suppose an observed set of data for supervised sub-class loss $f(\mathbf{x}_i, C_{\mathsf{sub},i}(fc_i, c_1, \ldots, c_K g))g_{i=1}^{M}$, where $C_{\mathsf{sub},i}$ is a subset of C such that $C_{\mathsf{sub},i}$ contains c_i of $\mathbf{x}_i$ and it holds 2 $jC_{\mathsf{sub},i}j$ $K+1$. We take derivatives of the empirical sub-class loss $\frac{1}{M}\sum_{i=1}^{M} \ \ln \frac{\exp(q_{c_i})}{\sum_{j2C_{\mathsf{sub},i}} \exp(q_j)}$ with respect to each element of $\mathbf{q}$, then the stationary points are $8c \ 2 \ C$,

$$\begin{aligned}
&\sum_{n_1 2 Cnc} N_{c,n_1} \left(1 \quad 2\frac{\exp(q_c)}{\sum_{j2fc,n_1 g} \exp(q_j)} \right) \\
&+ \sum_{n_1, n_2 2 Cnc} N_{c,n_1,n_2} \left(1 \quad 3\frac{\exp(q_c)}{\sum_{j2fc,n_1,n_2 g} \exp(q_j)} \right) \\
&\vdots \\
&+ \sum_{n_1, \ldots, n_K 2 Cnc} N_{c,n_1,\ldots,n_K} \left(1 \quad (K+1)\frac{\exp(q_c)}{\sum_{j2fc,n_1,\ldots,n_K g} \exp(q_j)} \right) = 0,
\end{aligned} \tag{25}$$

Table 3: The expected number of samples to draw all supervised classes.

Dataset	# classes	$\mathsf{E}[K+1]$
AGNews	4	9
CIFAR-10	10	30
CIFAR-100	100	519
ImageNet	1 000	7 709

where $N_{c,n_1,\ldots,n_K}$ is the frequency of $\mathsf{C}_{\mathsf{sub},i}$ such that $\sum_{i=1}^{M} \mathsf{I}[\mathsf{C}_{\mathsf{sub},i} = \mathsf{f}c_i\mathsf{g} \ [\ \mathsf{f}n_1,\ldots,n_K\mathsf{g}]$. As a result, the optimal $\mathbf{q}$ is a constant function with the same value. For supervised loss defined in Eq. (3), the optimal score function of class y is $q_y = \ln N_y + \mathrm{Constant}$, where N_y is the number of samples whose label is y and $\mathrm{Constant}$ 2 R. From the uniform assumption, the optimal $\mathbf{q}$ is the minimizer of L_{sup}. □

E Expected Number of Negative Samples to Draw all Supervised Labels

We assume that we sample a latent class from ρ independently. Let $\rho(c)$ 2 $[0,1]$ be a probability that c is sampled. Flajolet et al. [1992, Theorem 4.1] show the expected value of $K+1$ to sample all latent class in C is defined by

$$\mathsf{E}[K+1] = \int_0^1 \left(1 \quad \prod_{c2\mathsf{C}} [1 \quad \exp(\quad \rho(c)x)]\right) \mathrm{d}x. \tag{26}$$

Table 3 shows the expected number of sampled latent classes on a popular classification dataset when the latent class is the same as the supervised class. For ImageNet, we use the relative frequency of supervised classes in the training dataset as ρ. According to Table 3, the empirical number of negative samples is supposed to be natural, for example, K 8 096 in experiments by Chen et al. [2020a], He et al. [2020].

F Additional Experimental Results

F.1 Experimental Results related to Upper Bound of Collision Term in Corollary 9

As shown in Table 1, the upper bound values of the collision term did not increase by increasing K. We further analyzed representations in terms of the number of negative samples K.

As we discuss in the Section 4.2, we expect that cosine similar values between samples in the same latent class do not change by increasing K. To confirm that, Figures 2 and 3 show histgrams of cosine similarity values between all pairs of feature representations in the same supervised class. The cosine similarity values do not change by increasing K in practice. We used feature representation $\widehat{\mathbf{f}}(\mathbf{x})$ on the training dataset. We used the number of bins of each histogram as the square root of the number of cosine similarity values in each class. We did not use duplicated similarity values: similarity between $\widehat{\mathbf{f}}(\mathbf{x}_i)$ and $\widehat{\mathbf{f}}(\mathbf{x}_j)$, where i j. For the results of CIFAR-100 dataset on Figure 3, we show the histograms for the first 10 supervised classes due to the page width.

To understand more details of the feature representations, Figure 4 shows L2 norms of *unnormalized* feature representations extracted from the training data of CIFAR-10 and CIFAR-100. We used the same feature representation $\widehat{\mathbf{f}}(\mathbf{x})$ without L2 normalization as in Figures 2 and 3. Unlike cosine similarity and the collision upper bound values, the norm values increase by increasing K on CIFAR-10 with all K and CIFAR-100 with smaller K. We used the square root of the number of training samples, 223, as the number of bins of each histogram.

To show the tendency of cosine similarity and norms by increasing K, Figure 5 shows the relative change of a distance between histograms. Figure 5a shows the relative change values for the CIFAR-10 dataset based on Figures 2 and 4a. Similarity, Figure 5b shows the relative change values for the CIFAR-100 dataset based on Figures 3 and 4b. For the representations extracted from the CIFAR-10 dataset, we calculated the first Wasserstein distance between the histogram of $K+1 = 32$ and the

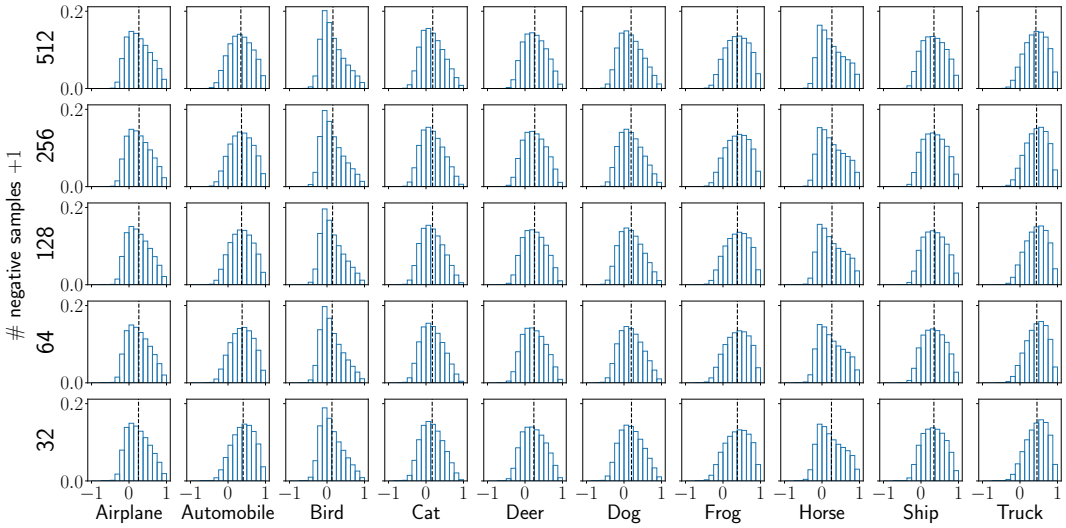

Figure 2: Histgrams of cosine similarity between the features in the same supervised class on CIFAR-10. The vertical lines represent the mean values.

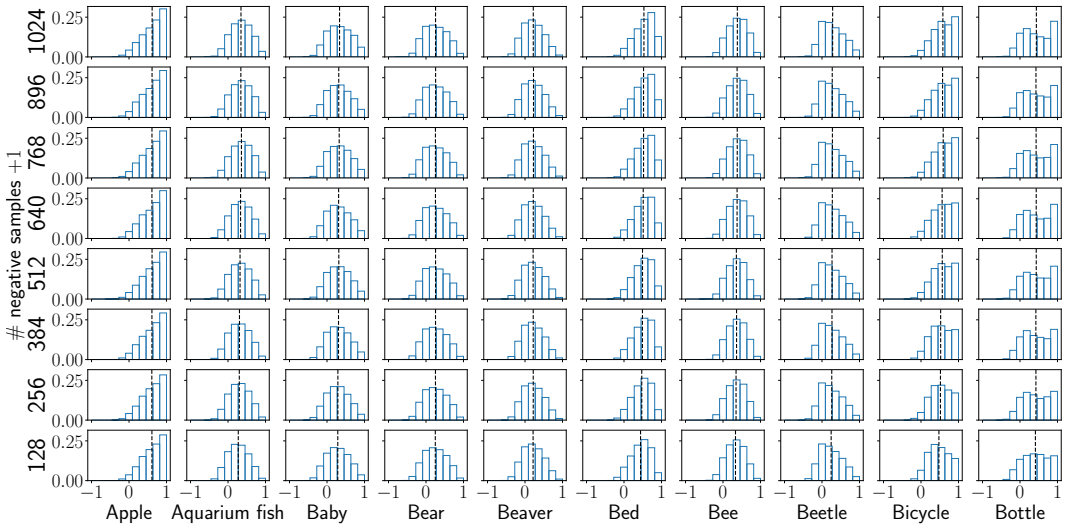

Figure 3: Histgrams of cosine similarity between the features in the same supervised class on CIFAR-100. The vertical lines represent the mean values.

other K values with Scipy [Virtanen et al., 2020]. We used the distance between the histograms of $K+1=32$ and $K+1=64$ as the reference value of the relative change. We calculated the averaged Wasserstein distance values among the supervised classes by random seed and took the averaged values over the three different random seeds. For CIFAR-100, we used the Wasserstein distance between histograms of $K+1=128$ and $K+1=256$ as the reference value. Note that we used minimum and maximum norm values to unify the range of histograms among different K since L2 norm values are not bounded above.

F.2 Details of Collision bound Calculation on Table 1

To calculate the upper bound (11) of the collision term without coefficient terms α, β, we sampled two data augmentations $\mathbf{a}$ and $\mathbf{a}^+$ per each training sample $\mathbf{x}$. The data augmentation distribution

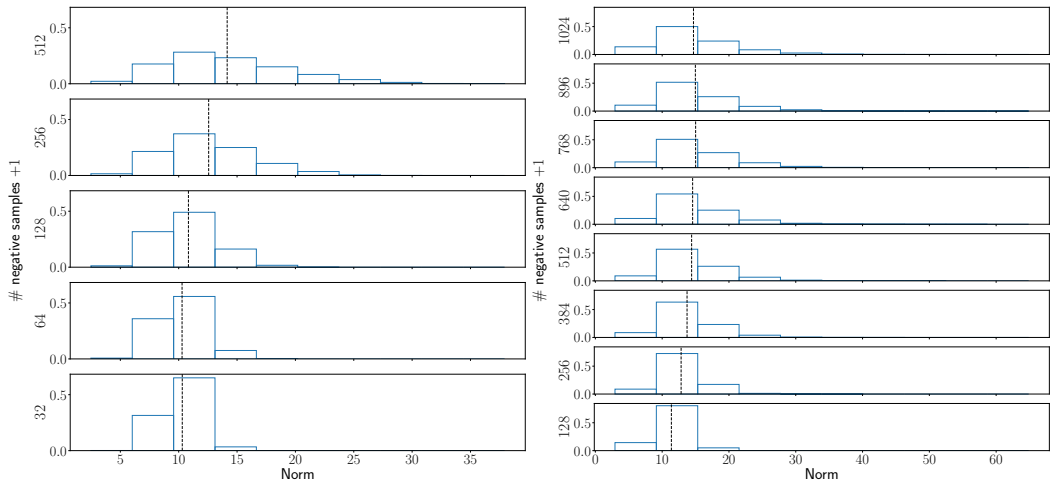

(a) CIFAR-10 (b) CIFAR-100

Figure 4: Histgrams of L2 norm values of unnormalized feature representations. The vertical lines represent the mean values.

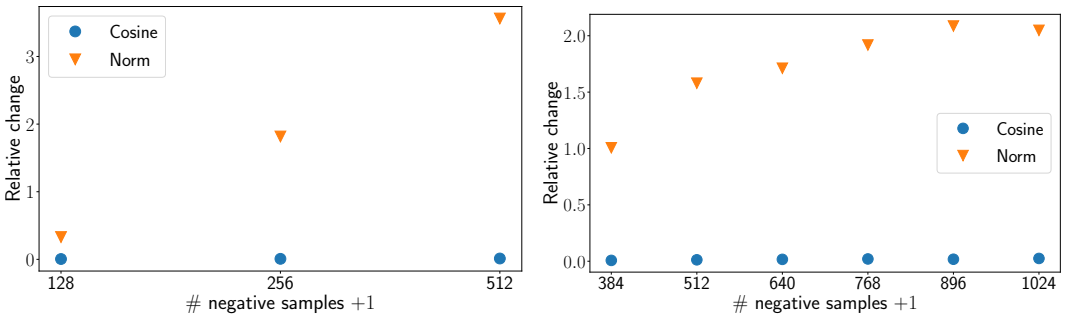

(a) Relative change of the first Wasserstein distance between the histogram of $K + 1 = 32$ and the histogram of the other $K + 1$ on CIFAR-10. The reference value is the distance between the histograms of $K + 1 = 32$ and $K + 1 = 64$.

(b) Relative change of the first Wasserstein distance between the histogram of $K + 1 = 128$ and the histogram of the other $K + 1$ on CIFAR-100. The reference is the distance between the histograms of $K + 1 = 128$ and $K + 1 = 256$.

Figure 5: Relative change of the first Wasserstein distance between histograms by increasing the number of negative samples.

was the same as described in Section 5. We approximated the upper bound term as follows:

$$\frac{1}{N}\sum_{i=1}^{N}\frac{1}{N_{y_i}}\sum_{j\neq i}^{N}\mathsf{I}\left[y_i = y_j\right] \quad \left|\mathbf{f}(\mathbf{a}_i(\mathbf{x}_i)) \quad \left[\mathbf{f}(\mathbf{a}_j(\mathbf{x}_j)) \quad \mathbf{f}(\mathbf{a}_i^{+}(\mathbf{x}_i))\right]\right|, \tag{27}$$

where recall that N_y is the number of samples whose label is y. We reported the averaged value of Eq. (27) with respect to the random seeds on Table 1.

F.3 Comprehensive Results of Table 1

Tables 4 and 5 show the comprehensive results of Table 1 for CIFAR-10 and CIFAR-100, respectively. Figure 6a shows upper bounds of supervised loss and the linear accuracy on the validation dataset.

F.4 Experiments on Natural Language Processing

Arora et al. [2019] conducted experiments for contrastive unsupervised sentence representation learning on Wiki-3029 dataset that contains 3 029 classes. However, we cannot use this dataset to perform similar experiments to CIFAR-10/100. This is because we need a huge number of negative

Table 4: The bound values on CIFAR-10 experiments with different $K+1$. CURL bound and its quantities are shown with y. The proposed ones are shown without y. Since the proposed collision values are half of ^{y}Collision, they are omitted. The reported values contain their coefficient except for Collision bound.

$K+1$		32	64	128	256	512
τ		0.96	1.00	1.00	1.00	1.00
υ		0.69	0.99	1.00	1.00	1.00
μ acc		72.75	75.30	77.22	78.60	80.12
Linear acc		77.13	79.70	81.33	82.85	84.13
Linear acc w/o		82.02	83.88	85.43	86.68	87.66
L_{Info}	Eq. (2)	2.02	2.64	3.29	3.96	4.64
$d(\mathbf{f})$	Eq. (7)	1.16	1.17	1.18	1.18	1.19
${}^{y}L_{\mathsf{Info}}$ bound	Eq. (8)	0.23	0.76	1.41	2.08	2.75
^{y}Collision		1.32	1.93	2.58	3.26	3.94
${}^{y}L^{\mu}_{\mathsf{sup}}$		0.05	0.00	0.00	0.00	0.00
${}^{y}L^{\mu}_{\mathsf{sub}}$		0.01	0.00	0.00	0.00	0.00
L_{Info} bound	Eq. (10)	0.39	0.70	1.02	1.35	1.69
L^{μ}_{sup}		0.63	0.90	0.91	0.90	0.90
L^{μ}_{sub}		0.26	0.01	0.00	0.00	0.00
Collision bound	Eq. (11)	0.60	0.61	0.61	0.62	0.62

Table 5: The bound values on CIFAR-100 experiments with different $K+1$. CURL bound and its quantities are shown with y. The proposed ones are shown without y. Since the proposed collision values are half of ^{y}Collision, they are omitted. The reported values contain their coefficient except for Collision bound.

$K+1$		128	256	384	512	640	768	896	1024
τ		0.72	0.92	0.98	0.99	1.00	1.00	1.00	1.00
υ		0.00	0.00	0.15	0.62	0.90	0.98	1.00	1.00
μ acc		32.74	34.22	35.27	35.98	36.58	37.10	36.84	37.50
Linear acc		42.01	43.59	44.28	45.09	45.72	46.06	45.50	46.52
Linear acc w/o		57.92	58.91	59.51	59.30	59.35	59.62	59.11	59.46
L_{Info}	Eq. (2)	3.32	3.98	4.38	4.66	4.88	5.06	5.21	5.34
$d(\mathbf{f})$	Eq. (7)	0.99	0.98	0.97	0.97	0.96	0.95	0.96	0.95
${}^{y}L_{\mathsf{Info}}$ bound	Eq. (8)	0.72	0.47	0.58	0.79	0.98	1.15	1.29	1.43
^{y}Collision		0.69	1.15	1.48	1.73	1.93	2.10	2.24	2.37
${}^{y}L^{\mu}_{\mathsf{sup}}$		0.00	0.00	0.01	0.01	0.01	0.00	0.00	0.00
${}^{y}L^{\mu}_{\mathsf{sub}}$		1.02	0.30	0.07	0.01	0.00	0.00	0.00	0.00
L_{Info} bound	Eq. (10)	1.18	1.53	1.72	1.86	1.96	2.05	2.12	2.19
L^{μ}_{sup}		0.00	0.00	0.30	1.21	1.76	1.92	1.95	1.95
L^{μ}_{sub}		1.82	1.93	1.66	0.75	0.20	0.04	0.01	0.00
Collision bound	Eq. (11)	0.52	0.52	0.52	0.51	0.51	0.51	0.51	0.51

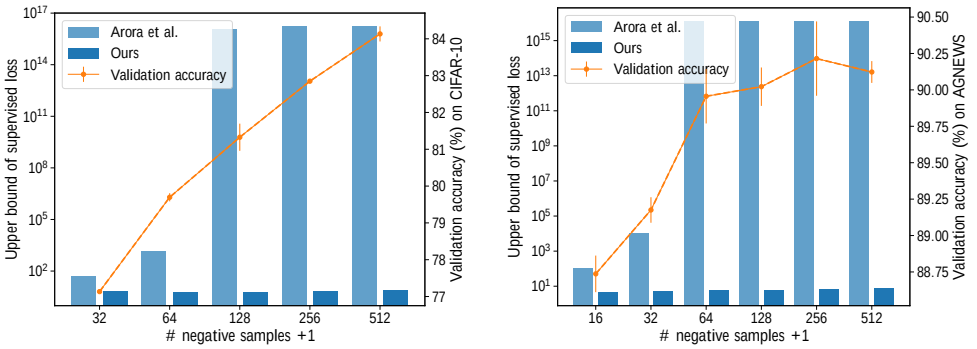

(a) CIFAR-10. (b) AGNews

Figure 6: Upper bounds of supervised loss and validation accuracy.

samples to perform the same control experiments as CIFAR-10/100's experiments from the coupon collector's problem. Concretely, we need to more than 26 030 negative samples from Eq. (26). Such large negative samples cause an optimization issue in practice. In addition, unlike self-supervised learning on vision, self-supervised learning algorithms on text do not use a large number of negative samples in practice. For example, Logeswaran and Lee [2018], Gao et al. [2021] use at most 399 and 1 023 negative samples in their experiments respectively.[13]

Dataset and Data Augmentation We used the AGNews classification dataset [Zhang et al., 2015] due to the aforementioned difficulty of the experiment on the Wiki-3029 dataset. The dataset contains 4 supervised classes and 120 000 training samples and 7 600 validation samples. As pre-processing, we used a tokenizer of torchtext with its default option: `basic_english`. After that, we removed words whose frequency was less than 5 in the training dataset. As a data augmentation, we randomly delete 20% words in each samples [Gao et al., 2021]. We tried a different data augmentation that randomly replaced 20% words with one of the predefined similar words inspired by Wang and Yang [2015]. To obtain similar words, we used the five most similar words in pre-trained word vectors on the Common Crawl dataset [Mikolov et al., 2018]. If a word in the training data of the AGNews dataset did not exist in the pre-trained word vector's dictionary, we did not replace the word.

Self-supervised Learning To compare the performance of supervised classification to the reported results on the AGNews dataset, we modify the supervised fastText model [Joulin et al., 2017] to model a feature encoder $\mathbf{f}$. The self-supervised model consists of a word embedding layer, an average pooling layer over the words, and the same nonlinear projection head as the CIFAR 10/100 experiment. The number of hidden units in the embedding layer and projection head was 50.

We only describe the difference from the vision experiment because we mainly follow the vision experiment. We trained the encoder by using PyTorch on a single GPU because the training was fast enough on a single GPU due to the model's simplicity. The number of epochs was 100. We used linear warmup at each step during the first 10 epochs. We did not apply weight decay by following Joulin et al. [2017]. For the base learning rate `lr` $\in \{1.0, 0.1\}$ and initialization of learning rate, either `lr` $\frac{K+1}{256}$ or `lr` $\sqrt{K+1}$, which are used in Chen et al. [2020a].

Linear Evaluation We followed the same optimization procedure as in the CIFAR 10/100 experiments except for the number of epochs that was 10 and performing single GPU training. We used the mean classifier's validation accuracy as a hyper-parameter selection criterion since we perform grid-search among two types of data augmentation, two learning rates, and two learning rate initialization methods. Note that the deletion data augmentation performed better than the replacement one.

Bound Evaluation Same as in the CIFAR 10/100 experiments except for $K + 1 \in \{32, 64, 128, 256, 512\}$ since the number of classes is 4.

[13] Precisely, all other samples in the same mini-batch are treated as negative samples.

Table 6: The bound values on AGNews experiments with different $K + 1$. CURL bound and its quantities are shown with y. The proposed ones are shown without y. Since the proposed collision values are half of ${}^{\mathsf{y}}$Collision, they are omitted. The reported values contain their coefficient except for Collision bound.

K + 1		16	32	64	128	256	512
τ		0.99	1.00	1.00	1.00	1.00	1.00
υ		0.96	1.00	1.00	1.00	1.00	1.00
μ acc		87.09	88.41	89.12	89.38	89.47	89.54
Linear acc		88.74	89.18	89.96	90.02	90.21	90.12
Linear acc w/o		87.11	87.94	89.05	89.49	89.62	89.45
L_{Info}	Eq. (2)	1.23	1.77	2.37	3.02	3.69	4.37
$d(\mathbf{f})$	Eq. (7)	1.72	1.77	1.81	1.82	1.83	1.84
${}^{\mathsf{y}}L_{\mathsf{Info}}$ bound	Eq. (8)	0.22	0.35	0.99	1.65	2.34	3.02
${}^{\mathsf{y}}$Collision		1.49	2.13	2.80	3.48	4.16	4.85
${}^{\mathsf{y}}L^{\mu}_{\mathsf{sup}}$		0.02	0.00	0.00	0.00	0.00	0.00
${}^{\mathsf{y}}L^{\mu}_{\mathsf{sub}}$		0.00	0.00	0.00	0.00	0.00	0.00
L_{Info} bound	Eq. (10)	0.39	0.10	0.22	0.55	0.89	1.23
L^{μ}_{sup}		0.57	0.61	0.63	0.64	0.64	0.65
L^{μ}_{sub}		0.02	0.00	0.00	0.00	0.00	0.00
Collision bound	Eq. (11)	0.87	0.89	0.91	0.92	0.93	0.93
${}^{\mathsf{y}}\ln L^{\mu}_{\mathsf{sup}}$ upper bound		4.72	9.28	37.06	37.05	37.04	37.04
$\ln L^{\mu}_{\mathsf{sup}}$ upper bound		1.52	1.60	1.72	1.83	1.93	2.02

Results Table 6 shows the quantities of bound-related values. When K was too small, both lower bounds were vacuous because an InfoNCE value should be non-negative. However, the lower bounds were negative. This vacuousness comes from $d(\mathbf{f})$ that takes negative value. Figure 6b shows the upper bound of mean classifier and linear accuracy on the validation dataset by rearranging InfoNCE's lower bounds. Figure 6b shows the similar tendency to Figure 1; by increasing K, the existing bound explodes, but the proposed bound does not.

Checklist

1. For all authors...
   (a) Do the main claims made in the abstract and introduction accurately reflect the paper's contributions and scope? [Yes]
   (b) Did you describe the limitations of your work? [Yes] See Section 7.
   (c) Did you discuss any potential negative societal impacts of your work? [No]
   (d) Have you read the ethics review guidelines and ensured that your paper conforms to them? [Yes]
2. If you are including theoretical results...
   (a) Did you state the full set of assumptions of all theoretical results? [Yes]
   (b) Did you include complete proofs of all theoretical results? [Yes] See Appendix D.1.
3. If you ran experiments...
   (a) Did you include the code, data, and instructions needed to reproduce the main experimental results (either in the supplemental material or as a URL)? [Yes] The experimental code and instructions are found in supplemental material.
   (b) Did you specify all the training details (e.g., data splits, hyperparameters, how they were chosen)? [Yes] See Section 5, where we used the original training and test splits for both CIFAR-10 and CIFAR-100 datasets. The hyper-parameters were chosen by following the experiments in Chen et al. [2020a].
   (c) Did you report error bars (e.g., with respect to the random seed after running experiments multiple times)? [Yes] The validation accuracy values on Figure 1 are shown with their standard deviation values.
   (d) Did you include the total amount of compute and the type of resources used (e.g., type of GPUs, internal cluster, or cloud provider)? [No] But Section 5 mentioned the type of GPUs was NVIDIA Tesla P100 on an internal cluster.
4. If you are using existing assets (e.g., code, data, models) or curating/releasing new assets...
   (a) If your work uses existing assets, did you cite the creators? [Yes] See Section 5, where we cited the creators of datasets and the libraries used in our experiments.
   (b) Did you mention the license of the assets? [Yes] The license of our experimental codes is the MIT license and it is as the anonymized license file in the supplimental material.
   (c) Did you include any new assets either in the supplemental material or as a URL? [Yes] We included the experimental codes in the supplimental material.
   (d) Did you discuss whether and how consent was obtained from people whose data you're using/curating? [N/A] We used CIFAR-10/100 datasets in our experiments.
   (e) Did you discuss whether the data you are using/curating contains personally identifiable information or offensive content? [N/A] We used CIFAR-10/100 datasets in our experiments.
5. If you used crowdsourcing or conducted research with human subjects...
   (a) Did you include the full text of instructions given to participants and screenshots, if applicable? [N/A]
   (b) Did you describe any potential participant risks, with links to Institutional Review Board (IRB) approvals, if applicable? [N/A]
   (c) Did you include the estimated hourly wage paid to participants and the total amount spent on participant compensation? [N/A]